Development/Plasticity/Repair

Genomewide Analysis of Rat Barrel Cortex Reveals Time- and Layer-Specific mRNA Expression Changes Related to Experience-Dependent Plasticity

Astrid Vallès,[1,2] Arjen J. Boender,[2] Steef Gijsbers,[2] Roy A. M. Haast,[2] Gerard J. M. Martens,[2]* and Peter de Weerd[1]*

[1]Department of Neurocognition, Faculty of Psychology and Neurosciences, Maastricht University, 6200 MD Maastricht, The Netherlands, and [2]Department of Molecular Animal Physiology, Radboud University Nijmegen, Donders Institute for Brain, Cognition, and Behaviour (Centre for Neuroscience), Nijmegen Centre for Molecular Life Sciences, 6525 GA Nijmegen, The Netherlands

Because of its anatomical organization, the rodent whisker-to-barrel system is an ideal model to study experience-dependent plasticity. Manipulation of sensory input causes changes in the properties of the barrels at the physiological, structural, and functional levels. However, much less is known about the molecular events underlying these changes. To explore such molecular events, we have used a genomewide approach to identify key genes and molecular pathways involved in experience-induced plasticity in the barrel cortex of adult rats. Given the natural tendency of rats to explore novel objects, exposure to an enriched environment (EE) was used to stimulate the activity of the whisker-to-barrel cortex *in vivo*. Microarray analysis at two different time points after EE revealed differential expression of genes encoding transcription factors, including nuclear receptors, as well as of genes involved in the regulation of synaptic plasticity, cell differentiation, metabolism, and, surprisingly, blood vessel morphogenesis. These expression differences reflect changes in somatosensory information processing because unilateral whisker clipping showed EE-induced differential expression patterns in the spared versus deprived barrel cortex. Finally, *in situ* hybridization revealed cortical layer patterns specific for each selected gene. Together, the present study offers the first genomewide exploration of the key genes regulated by somatosensory stimulation in the barrel cortex and thus provides a solid experimental framework for future in-depth analysis of the mechanisms underlying experience-dependent plasticity.

Introduction

Experience-dependent plasticity enables organisms to adapt their behavior to the environment. However, how experience shapes the functional organization of different brain systems is still poorly understood. At the level of sensory systems, the rodent primary somatosensory cortex (S1) is a particularly suited model to investigate the mechanisms underlying experience-dependent plasticity (Feldman and Brecht, 2005). The whisker-to-barrel system plays an important role in various types of rodent behavior, from foraging to object recognition (Brecht, 2007; Diamond et al., 2008). Its organization allows for the precise characterization of experience-dependent plasticity, thanks to the one-to-one correspondence of each whisker to its cortical receptive field in layer 4 of S1, the "barrel" (Woolsey and Van der Loos, 1970). In the barrel cortex, plasticity can be induced by modifying sensory input through simple manipulations, such as exposure to enriched environment (EE) or whisker clipping (Fox, 2002; Polley et al., 2004).

Because of its easy accessibility, the whisker-to-barrel system is an ideal model to integrate a wide range of experimental approaches to dissect plasticity mechanisms at different levels, such as genetics, molecular biology, electrophysiology, and imaging (Brecht et al., 2004; Schubert et al., 2007; Petersen, 2009). Most studies investigating experience-dependent plasticity in barrel cortex make use of electrophysiological methods (Petersen, 2007). More recently, gene targeting and viral vector strategies have also been applied, permitting layer- and column-specific manipulation of the expression of selected genes to study their function (Aronoff and Petersen, 2008), visualization of structural plasticity (Knott and Holtmaat, 2008), and control of neuronal activity to examine network connectivity and behavior through optogenetic approaches (Huber et al., 2008; Petreanu et al., 2009). For such studies, knowledge of the genes expressed in the barrel cortex both under resting conditions and after neuronal stimulation is of crucial importance, in particular of those induced by sensory experience and their cortical layer and cellular expression patterns.

A limited number of studies have determined the expression of selected genes in barrel cortex after activation of the whisker system. Single-whisker experience induces cAMP responsive element (CRE)-dependent gene expression in the spared barrel of transgene reporter mice (Barth et al., 2000), whereas neuritin, a plasticity-related gene, shows differential regulation in spared and deprived barrels (Harwell et al., 2005). Passive whisker stimulation increases brain-derived neurotrophic factor (*Bdnf*)

Received Dec. 14, 2010; revised Jan. 26, 2011; accepted Feb. 26, 2011.

This research was supported by VICI Grant 453_04_002 from the Netherlands Foundation of Scientific Research (P.d.W.). We thank Dr. Freddy de Bree for his valuable help with the bioinformatic analysis.

*G.J.M.M. and P.d.W. contributed equally to this work.

Correspondence should be addressed to Peter de Weerd, Department of Neurocognition, Faculty of Psychology and Neurosciences, Maastricht University, P.O. Box 616, 6200 MD Maastricht, The Netherlands. E-mail: p.deweerd@maastrichtuniversity.nl.

DOI:10.1523/JNEUROSCI.6514-10.2011

 0270-6474/11/316140-19$15.00/0

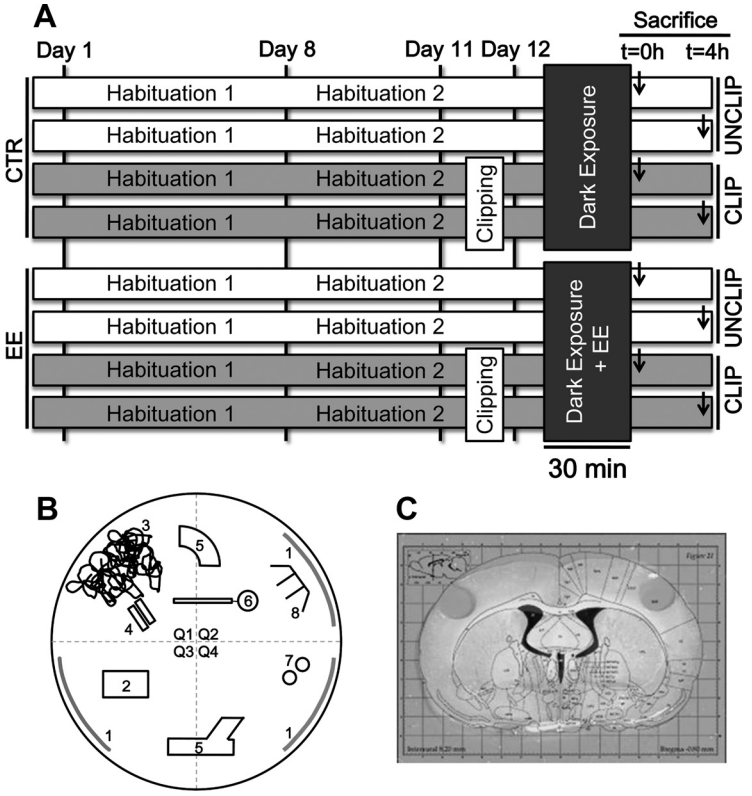

Figure 1. Overview of the experimental design and methods of tissue dissection. ***A***, General experimental design. The animals underwent a first habituation period for 7 d, followed by a second habituation period of 5 d. On day 11, the right whiskers of half of the rats were clipped (CLIP) under anesthesia; the other half received anesthesia only (UNCLIP). On day 12, the animals were exposed to the dark, with or without exposure to EE for 30 min (EE and CTR groups, respectively) and killed either immediately ($t = 0$ h) or 4 h ($t = 4$ h) after the end of the experiment. ***B***, Enriched environment cage. The cage in which the rats were placed for a period of 30 min. Shown are the EE attributes (1–8) and the quadrants (Q1–Q4). The EE objects used were (1) different textures, (2) grated plastic box, (3) curled paper, (4) foam pipes, (5) plastic pipes, (6) wooden brush, (7) plastic balls, and (8) plastic wire strainer. Care was taken to place these objects always in the same place at the beginning of the EE session. ***C***, Dissection area. The barrel cortex was dissected, separately for left and right hemispheres, using a 2 mm micropunch. Shown is the remaining tissue after micropunch, overlaid to its corresponding stereotactic picture (Paxinos and Watson, 1998) showing that the area was always located in S1 and spanned layers 1–6.

(Rocamora et al., 1996), synaptophysin (Ishibashi, 2002), and mRNA of glial glutamate transporters (Genoud et al., 2006). In addition, sensory experience, such as EE, induces expression of the immediate-early genes cAMP responsive element modulator (*Crem*), *Fos*, *JunB*, and early-growth response 1 (*Egr1*) (Filipkowski et al., 2001; Bisler et al., 2002). However, a genomewide study on genes activated during sensory experience has not been performed yet. In the present study, we used microarray analysis and validation by quantitative PCR (qPCR) and *in situ* hybridization in combination with whisker clipping experiments to explore global EE-induced mRNA expression patterns in the barrel cortex of adult rats. A number of differentially expressed genes were identified, providing novel insights into the molecular cascades responsive to experience-dependent plasticity in the rodent somatosensory system.

Materials and Methods

Animals. Male Long–Evans rats (Harlan) were used, ranging in age from 65 to 75 d. A total of $n = 36$ animals were used for microarray and qPCR analysis (group size, $n = 6–8$) and $n = 24$ for *in situ* hybridization experiments (group size, $n = 4$). The animals were housed two per cage (37.8 × 21.7 × 18.0 cm) in a controlled environment under a 12 h light/dark cycle with lights on at 6:30 A.M. Food and water were provided *ad libitum*. Experimental procedures were performed between 7:30 A.M. and 2:30 P.M. All the experimental groups were constructed using matched weight criteria. The experiments were approved by the Animal Ethics Committee of the Radboud University Nijmegen (Nijmegen, The Netherlands), according to Dutch legislation.

Experimental procedure. A schematic overview of the experimental procedure is depicted in Figure 1*A*. To reduce stress levels, all rats underwent two habituation periods. During the first period, lasting 7 d, the rats were handled and weighed daily. In the second period, lasting 5 d, the rats were placed per two in the empty test cage (round, plastic cage; 0.88 m^2) for 30 min on a daily basis. Note that two rats from the same home cage were placed together in the test cage and not individually or in a larger group, to avoid stress caused by isolation or by exposure to "stranger" rats (rats from other home cages). To prevent any visual stimulation and promote mainly the use of the somatosensory system, the test cage was located in a room without illumination. The procedures to which the rats were subjected during the five habituation sessions in the empty test cage during the second habitation period were identical to the procedures applied during the actual EE session. Because of this, stress during the EE session can be assumed to be very low. For clarity, the habituation sessions are not part of the sensory enrichment manipulation. After the habituation period, all the rats underwent a short (2–3 min) 2% isoflurane mixed gas O_2 anesthesia (Pharmachemie BV). During anesthesia, the right whiskers of half of the animals were clipped as close to the skin as possible (CLIP), whereas the whiskers of the other rats were left intact (UNCLIP). The following day, both groups were transferred to a room without illumination, where they either stayed in their home cage (CTR) or were allowed to explore the enriched test cages, per two (EE), in a single session of 30 min. Exploration of the EE took place in the dark to increase somatosensory (vs visual) stimulation. The objects used for enrichment are depicted in Figure 1*B*; the position of the objects was kept as similar as possible between the tests. To quantify behavior (see below, Behavioral analysis), all sessions were videotaped using infrared cameras (Velleman). The animals from the experimental (EE) group consistently displayed high levels of activity. In contrast, we observed that, most of the time, CTR animals were inactive in their home cage, and therefore the behavior of CTR animals was not quantified. For microarray and qPCR analysis, the rats were decapitated either immediately after the end of the EE session ($t = 0$ h) or 4 h later ($t = 4$ h). After decapitation, the brains were carefully dissected, frozen on dry ice, and stored at −80°C until additional analysis. For *in situ* hybridization analysis, CTR animals were killed immediately ($t = 0$ h), whereas EE animals were killed either immediately ($t = 0$ h) or 4 h ($t = 4$ h) after enrichment. The animals were killed by terminal anesthesia with sodium pentobarbital (90 mg/kg, i.p.), followed by intracardiac perfusion with ice-cold 0.9% saline for 1–2 min and perfusion fixation with 4% ice-cold paraformaldehyde (PFA), pH 7.4, for 10 min (perfusion rate, 25–30 ml/min). The brains were dissected, postfixed overnight in 4% PFA at 4°C, and transferred to 30% sucrose in PBS at 4°C until sectioning.

Behavioral analysis. The behaviors of all EE animals (both UNCLIP and CLIP groups) were quantified using The Observer 5.0 (Noldus Information Technology). A period of 10 min was analyzed, starting 10 min after the beginning of the EE exposure. The behavior was divided into six different categories, namely "fighting," "gnawing," "grooming," "rear-

Table 1. Primers for quantitative PCR

Gene	Forward primer (5′–3′)	Reverse primer (5′–3′)	Amplicon size (bp)
Abcg2	TTCTCATGACGATCTCTTTTGTGTT	CATATCGAGGAATGCTAAAGTACTGAA	114
Apold1	CGGGTCCAGCTCTGTACCA	GCTGCGAATCTAGAACATTCCA	121
Arc	CCGTCCCCTCCTCTCTTGA	AAGGCACCTCCTCTTTGTAATCCTAT	89
BDNF	GGTCACAGCGGCAGATAAAAAGAC	TTCGGCATTGCGAGTTCCAG	188
Btg2	TCCTGAGGACTCGGGGCTGC	GCGATAGCCGGAGCCCTTGG	131
Fos	TCCCAGCTGCACTACCTATACGT	TGCGCAGCTAGGGAAGGA	73
Ch25h	CCGTTTGGCTGGTACGGGGG	CAGGCGCTTCGAGTGGGGTG	135
Chrm4	AGAGTGCCCTGCTAATGTTGCT	CTAATTGACTCAGTGCCCTGGAA	145
CycA	**AGCACTGGGGAGAAAGGATT**	**AGCCACTCAGTCTTGGCAGT**	**248**
Cyr61	AACTCGGAGTGCCGCCTGGT	GCCGCAGTATTTGGGCCGGT	183
Dusp1	AGGACAACCACAAGGCAGACA	CCAGCATCCTTGATGGAGTCTAT	76
Egr3	AAGCGCCACGCCAAGAT	GGCGCCGAGGATGCA	80
FosB	ACGCACCCCCCAACCT	AGGAAGTGTACGAAGGGCTAACA	96
Nptx2	AGCGTCTCCTGGACTTGTAGCTA	TCGGGAATAGATGCCTTGAACT	87
Nr4a2	CATTTCTGCCTTCTCCTGCATT	AAGTCACATGGTCTTTAAGACAAGACAATTTACA	125
Pcsk1	AATCTCACCTGGCGAGATATGC	ATCAAGCCCGCTCCATTCT	101
Pde7b	CGCGCTGGGTTTCGAA	GCTTTTGTACACTTGGATCAACGA	72
Plat	GCAGGGAAGTATACCACGGAGTT	TGGGTGCCACGGTAAGTCA	100
Prom1	CTTCTTTTGTATGTGCCGTTGCT	AACGCGATGCCAAGACTCA	141
Ywhaz	**TTGAGCAGAAGACGGAAGGT**	**GAAGCATTGGGGATCAAGAA**	**136**
β-Actin	**CGTGAAAAGATGACCCAGATCA**	**AGAGGCATACAGGGACAACACA**	**89**

Shown are the names of the genes selected for qPCR analysis, the sequences of the forward and reverse primers from 5′ to 3′, and the size of the final product. The tested housekeeping genes are in bold.

Table 2. Primers for probe template generation (*in situ* hybridization)

Genes	External primers (5′–3′)	Internal primers (5′–3′)	Amplicon size (bp)
Apold1			
Forward		**AATTAACCCTCACTAAAGGG**TCTCTCTGATCTTCTGCAATTCCC	301
Reverse		**TAATACGACTCACTATAGGG**TCCAGGCTCTCAGACAGTTTCTG	
Egr3			
Forward	CTTTCCAGCCAGCCCCAGGC	**AATTAACCCTCACTAAAGGG**GAGTGCCGGCATCTTGGGGG	601
Reverse	CGGTGTGCGTGCGGATGTGA	**TAATACGACTCACTATAGGG**CTGGAAGGGCTTGTGGCCCG	
Nr4a2			
Forward	CAAGGAGCCAGCCCCGCTTC	**AATTAACCCTCACTAAAGGG**TCAGATGCACAACTACCAGCAAC	1001
Reverse	GCCACGCACGCATTGCAACC	**TAATACGACTCACTATAGGG**CAGCAAAGCCAGGAATCTTCTCT	
Ch25h			
Forward	AAGGACGGGAGAGGCGTCCG	**AATTAACCCTCACTAAAGGG**TCAGATGCACAACTACCAGCAAC	653
Reverse	ACAGGCGCTTCGAGTGGGGT	**TAATACGACTCACTATAGGG**CAGCAAAGCCAGGAATCTTCTCT	
Btg2			
Forward	TCCTGAGGACTCGGGGCTGC	**AATTAACCCTCACTAAAGGG**GGTTTTCAGTAGGGCGCTCCAGG	305
Reverse	TGGACTGCTCCTGCCCAGCAT	**TAATACGACTCACTATAGGG**GGCTGGGAGGCCCAGTTCCA	
Cyr61			
Forward	ACTCTCCACCTGCCCTGCCG	**AATTAACCCTCACTAAAGGG**CCCGGGAGTCGGCTTGGTCC	326
Reverse	TTCCTCACAGCACTGCCCGC	**TAATACGACTCACTATAGGG**GGGGGTTGGGACAGCCCAGA	
Nptx2			
Forward		**AATTAACCCTCACTAAAGGG**TCACCGGCAGAAGACAGAGAAC	605
Reverse		**TAATACGACTCACTATAGGG**AGCAGTTGGCGATGTTGATGAT	
Fos			
Forward	AACTTTATCCCCACGGTGACAG	**AATTAACCCTCACTAAAGGG**AGAATCCGAAGGGAAAGGAATA	702
Reverse	TGAACATGGACGCTGAAGAGC	**TAATACGACTCACTATAGGG**AGCTCAGTGAGTCAGAGGAGGG	

Shown are the names of the genes selected for *in situ* hybridization, the sequences of the forward and reverse external and internal primers from 5′ to 3′, and the size of the final product after the second (internal) PCR reaction. The T3 (5′AATTAACCCTCACTAAAGGG3′) and T7 (5′TAATACGACTCACTATAGGG3′) RNA polymerase sequences at the 5′ of the internal forward and reverse primers are highlighted in bold. The Arc plasmid containing the full-length rat Arc cDNA subcloned into the EcoRI–XhoI site of pBluescriptII SK+ (Stratagene) was provided by Dr P. F. Worley (John Hopkins University). The plasmid was linearized with EcoRI or XhoI and transcribed with T7 or SP6 RNA polymerases to generate antisense and sense probes, respectively.

ing," "whisking," and a final category with all other behaviors, called "other." The time spans of these different categories were measured. Next to this, the cage was divided into different quadrants (Fig. 1*B*), and the total time spent in these quadrants was also quantified. Levene's test was performed to test the homogeneity of the data. In case of non-homogeneous data, a log transformation was executed. Subsequently, two-way ANOVAs (with "behavior" and "clipping" or "behavior" and "quadrant" as factors), followed by Student–Newman–Keuls (SNK) *post hoc* analyses when appropriate, were performed, with a significance level of $p \leq 0.05$. All tests were executed using SPSS 17.0 (SPSS Inc.).

Tissue processing. All procedures were performed under RNase-free conditions. For microarray and quantitative PCR analysis, the brains were sliced into 300 μm coronal sections using a cryotome (Leica) at −15°C and mounted on glass slides. Cytochrome oxidase-stained reference sections were used as a template to locate the barrel cortex, following stereotactic coordinates (Paxinos and Watson, 1998). Punches of barrel cortex (Fig. 1*C*) were taken bilaterally using a 2 mm micropunch (Harris Inc.), and samples from each hemisphere were collected separately and stored at −80°C before RNA isolation took place. For *in situ* hybridization, the brains were sliced into 40 μm coronal sections using a sliding microtome (Microm HM440E; Thermo Fisher Scientific). Sections were stored at −20°C in cryoprotectant

Table 3. List of differentially expressed genes identified by microarray after EE, ordered by *q* value (smallest to largest)

Affymetrix transcripts cluster ID	Gene symbol	Gene title	SAM *q* value	FC $t = 0$ h		FC $t = 4$ h	
10767767	Btg2	BTG family, member 2	8.78E-08	5.01	Up	1.16	Up
10899387	Nr4a1	Nuclear receptor subfamily 4, group A, member 1	8.78E-08	3.14	Up	1.11	Up
10904511	Arc	Activity-regulated cytoskeleton-associated protein	8.78E-08	2.38	Up	1.35	Up
10732652	Dusp1	Dual specificity phosphatase 1	1.32E-07	3.26	Up	1.06	Up
10827231	Cyr61	Cysteine-rich, angiogenic inducer, 61	3.07E-07	6.48	Up	1.10	Up
10859262	Apold1	Apolipoprotein L domain containing 1	3.51E-07	6.45	Up	1.10	Up
10727717	Npas4	Neuronal PAS domain protein 4	3.51E-07	4.95	Up	1.10	Up
10832802	Egr2	Early growth response 2	3.51E-07	3.73	Up	1.07	Down
10886031	Fos	FBJ osteosarcoma oncogene	7.91E-07	3.78	Up	1.05	Down
10720215	Zfp36	Zinc finger protein 36	8.78E-07	3.10	Up	1.06	Up
10832197	Sik1	Salt-inducible kinase 1	1.01E-06	2.47	Up	1.02	Down
10868940	Nr4a3	Nuclear receptor subfamily 4, group A, member 3	1.10E-06	2.68	Up	1.14	Up
10845384	Nr4a2	Nuclear receptor subfamily 4, group A, member 2	1.14E-06	3.20	Up	2.02	Up
10806585	JunB	JunB proto-oncogene	1.23E-06	2.86	Up	1.14	Down
10815763	Tiparp	TCDD-inducible poly(ADP-ribose) polymerase	1.45E-06	2.75	Up	1.17	Down
10800919	Egr1	Early growth response 1	1.45E-06	1.61	Up	1.10	Up
10909360	Snord14	Small nucleolar RNA SNORD14	1.58E-06	3.43	Up	1.20	Down
10878112	Jun	Jun oncogene	1.63E-06	2.07	Up	1.11	Down
10734882	Per1	Period homolog 1 (*Drosophila*)	1.80E-06	1.65	Up	1.02	Down
10770710	Atf3	Activating transcription factor 3	2.02E-06	2.05	Up	1.23	Up
10900358	Gadd45b	Growth arrest and DNA-damage-inducible, β	2.28E-06	1.90	Up	1.10	Up
10735866	rno-mir-212	miR-212 stem-loop	2.77E-06	1.89	Up	1.12	Up
10719432	FosB	FBJ osteosarcoma oncogene B	2.90E-06	2.08	Up	1.07	Up
10796543	Arl5b	ADP-ribosylation factor-like 5B	2.94E-06	1.75	Up	1.10	Up
10792421	Plat	Plasminogen activator, tissue	3.03E-06	1.74	Up	1.10	Down
10743966	Kdm6b	Lysine (K)-specific demethylase 6B	3.03E-06	1.40	Up	1.08	Up
10896793	Trib1	Tribbles homolog 1 (*Drosophila*)	3.12E-06	1.93	Up	1.14	Up
10909356	Snord14	Small nucleolar RNA SNORD14	3.38E-06	2.75	Up	1.13	Down
10790670	Klf2	Kruppel-like factor 2 (lung)	3.69E-06	1.42	Up	1.04	Down
10737506	Tob1	Transducer of ErbB-2.1	3.78E-06	1.53	Up	1.11	Down
10729777	Ch25h	Cholesterol 25-hydroxylase	4.04E-06	1.75	Up	1.13	Up
10909358	Snord14	Small nucleolar RNA SNORD14	4.57E-06	2.09	Up	1.19	Up
10895144	Dusp6	Dual specificity phosphatase 6	4.70E-06	1.72	Up	1.01	Down
10923338	Coq10b	Coenzyme Q10 homolog B (*Saccharomyces cerevisiae*)	4.83E-06	1.74	Up	1.07	Up
10796147	U6	U6 spliceosomal RNA	5.01E-06	1.55	Up	1.02	Up
10806685	Ier2	Immediate early response 2	5.23E-06	1.83	Up	1.30	Up
10797527	Gadd45g	Growth arrest and DNA-damage-inducible, γ	5.23E-06	1.65	Up	1.20	Up
10799241	Idi1	Isopentenyl-diphosphate Δ isomerase 1	5.84E-06	1.46	Up	1.03	Down
10823508	Ccnl1	Cyclin L1	5.97E-06	1.58	Up	1.09	Down
10923866	Zdbf2	Zinc finger, DBF-type containing 2	6.28E-06	1.59	Up	1.33	Up
10744376	Bcl6b	B-cell CLL/lymphoma 6, member B (zinc finger protein)	6.50E-06	1.51	Up	1.11	Up
10781337	Egr3	Early growth response 3	6.50E-06	1.51	Up	1.80	Up
10878938	Plk3	Polo-like kinase 3 (*Drosophila*)	6.90E-06	1.64	Up	1.02	Up
10873578	Snora15	Small nucleolar RNA SNORA15	7.42E-06	1.74	Up	1.11	Down
10721865	Ppp1r15a	Protein phosphatase 1, regulatory (inhibitor) subunit 15A	8.35E-06	1.74	Up	1.06	Down
10903998	U6	U6 spliceosomal RNA	8.39E-06	1.98	Up	1.08	Down
10795616	Crem	cAMP responsive element modulator	9.40E-06	1.51	Up	1.29	Up
10774375	Peli1	Pellino 1	9.53E-06	1.34	Up	1.10	Down
10861986	Insig1	Insulin induced gene 1	9.53E-06	1.23	Up	1.10	Down
10731193	rno-mir-212	rno-mir-212 stem-loop	9.66E-06	1.61	Up	1.03	Down
10834447	Egfl7	EGF-like-domain, multiple 7	1.04E-05	1.41	Up	1.00	Up
10788483	Lonrf1	LON peptidase N-terminal domain and ring finger 1	1.18E-05	1.33	Up	1.15	Down
10820666	Hmgcr	3-Hydroxy-3-methylglutaryl-coenzyme A reductase	1.26E-05	1.32	Up	1.01	Up
10822330	Zbtb10	Zinc finger and BTB domain containing 10	1.28E-05	1.48	Up	1.11	Down
10773115	Prom1	Prominin 1	1.31E-05	1.00	Up	1.64	Down
10876838	Klf4	Kruppel-like factor 4 (gut)	1.33E-05	1.53	Up	1.06	Up
10824409	U6	U6 spliceosomal RNA	1.48E-05	1.59	Up	1.19	Down
10760290	Nptx2	Neuronal pentraxin 2	1.49E-05	1.18	Up	1.45	Up
10764551	Ptgs2	Prostaglandin-endoperoxide synthase 2	1.59E-05	1.61	Up	1.01	Down
10873814	Klf4	Kruppel-like factor 4 (gut)	1.60E-05	1.77	Up	1.06	Up
10752839	Adamts1	ADAM metallopeptidase with thrombospondin type 1 motif, 1	1.66E-05	1.43	Up	1.12	Up
10817552	Txnip	Thioredoxin interacting protein	1.87E-05	1.29	Up	1.29	Down
10702025	Ahi1	Abelson helper integration site 1	1.87E-05	1.28	Up	1.07	Down
10837998	Chrm4	Cholinergic receptor, muscarinic 4	1.96E-05	1.34	Up	1.01	Down

Table continued

Table 3. *Continued*

Affymetrix transcripts cluster ID	Gene symbol	Gene title	SAM *q* value	FC $t = 0$ h		FC $t = 4$ h	
10855862	Abcg2	ATP-binding cassette, subfamily G (WHITE), member 2	2.20E-05	1.06	Up	1.40	Down
10900318	Snord37	Small nucleolar RNA SNORD37	2.27E-05	1.62	Up	1.37	Down
10789653	Irs2	Insulin receptor substrate 2	2.33E-05	1.36	Up	1.10	Up
10727806	Snora19	Small nucleolar RNA SNORA19	2.39E-05	1.46	Up	1.08	Down
10923270	Obfc2a	Oligonucleotide/oligosaccharide-binding fold containing 2A	2.80E-05	1.29	Up	1.16	Down
10812184	Pcsk1	Proprotein convertase subtilisin/kexin type 1	2.89E-05	1.33	Up	1.16	Up
10714973	Hectd2	HECT domain containing 2	2.90E-05	1.21	Up	1.05	Down
10875322	Son	Son DNA binding protein	3.08E-05	1.14	Up	1.36	Down
10738477	Arl4d	ADP-ribosylation factor-like 4D	3.18E-05	1.32	Up	1.04	Up
10844339	Slc25a25	Solute carrier family 25 (mitochondrial carrier, phosphate carrier), member 25	3.19E-05	1.31	Up	1.13	Down
10933716	Sat1	Spermidine/spermine N1-acetyl transferase 1	3.40E-05	1.34	Up	1.04	Down
10861658	LOC688916	Hypothetical protein LOC688916	3.47E-05	1.21	Up	1.02	Down
10867033	Slco1a4	Solute carrier organic anion transporter family, member 1a4	3.49E-05	1.03	Down	1.40	Down
10720859	Fxyd5	FXYD domain-containing ion transport regulator 5	3.53E-05	1.09	Down	1.41	Up
10713604	Snord30	Small nucleolar RNA SNORD30	3.59E-05	1.35	Up	1.31	Down
10920967	Csrnp1	Cysteine-serine-rich nuclear protein 1	3.84E-05	1.33	Up	1.17	Up
10742245	U6	U6 spliceosomal RNA	3.99E-05	1.38	Up	1.04	Down
10905521	Pdgfb	Platelet-derived growth factor β polypeptide	4.42E-05	1.21	Up	1.05	Down
10717069	Pde7b	Phosphodiesterase 7B	4.55E-05	1.03	Up	1.51	Up
10842341	Trp53rk	TP53 regulating kinase	4.58E-05	1.18	Up	1.27	Up
10936263	Zbtb33	Zinc finger and BTB domain containing 33	4.69E-05	1.36	Up	1.06	Up
10887080	rno-mir-376a	rno-mir-376a stem-loop	4.74E-05	1.46	Up	1.14	Down
10899187	Gpd1	Glycerol-3-phosphate dehydrogenase 1 (soluble)	4.77E-05	1.20	Up	1.30	Down
10755670	U6	U6 spliceosomal RNA	4.99E-05	1.12	Up	1.49	Down
10794225	Nfil3	Nuclear factor, interleukin 3 regulated	5.02E-05	1.23	Up	1.10	Up
10713602	Snord28	Small nucleolar RNA SNORD28	5.07E-05	1.47	Up	1.10	Down
10932310	Med14	Mediator complex subunit 14	5.25E-05	1.41	Up	1.02	Down
10928229	Clk1	CDC-like kinase 1	5.66E-05	1.31	Up	1.13	Down
10744141	Snora67	Small nucleolar RNA SNORA67	6.04E-05	1.46	Up	1.13	Down
10863221	Mat2a	Methionine adenosyltransferase II, α	6.65E-05	1.25	Up	1.25	Down
10796673	Otud1	OTU domain containing 1	6.84E-05	1.30	Up	1.07	Up
10861617	Rcn1	Reticulocalbin 1, EF-hand calcium binding domain	6.97E-05	1.21	Down	1.09	Down
10798702	Inhba	Inhibin β-A	7.31E-05	1.02	Up	1.42	Up
10754642	Snora36	Small nucleolar RNA SNORA36 family	7.42E-05	1.28	Up	1.10	Down
10853300	Abcb1a	ATP-binding cassette, subfamily B (MDR/TAP), member 1A	7.64E-05	1.05	Up	1.37	Down
10891594	Foxn3	Forkhead box N3	8.26E-05	1.12	Up	1.24	Down
10862747	Spty2d1	SPT2, suppressor of Ty, domain containing 1 (*S. cerevisiae*)	8.63E-05	1.38	Up	1.09	Down
10844962	Lrp1b	Low-density lipoprotein-related protein 1B (deleted in tumors)	9.37E-05	1.11	Up	1.41	Down
10714903	Ifit3	Interferon-induced protein with tetratricopeptide repeats 3	9.42E-05	1.41	Up	1.03	Up
10717331	Sgk1	Serum/glucocorticoid regulated kinase 1	9.43E-05	1.29	Up	1.07	Down
10852620	Bdnf	Brain-derived neurotrophic factor	1.02E-04	1.28	Up	1.20	Up
10820108	Ankrd32	Ankyrin repeat domain 32	1.04E-04	1.19	Up	1.36	Down
10726308	Mettl10	Methyltransferase like 10	1.06E-04	1.06	Up	1.41	Down
10803947	Hbegf	Heparin-binding EGF-like growth factor	1.12E-04	1.40	Up	1.11	Up
10767001	Mat2a	Methionine adenosyltransferase II, α	1.14E-04	1.28	Up	1.25	Down
10880562	LOC364562	Similar to peptidyl-prolyl *cis*-trans isomerase A (PPIase) (Rotamase)	1.17E-04	1.06	Up	1.44	Up
10891402	Dio2	Deiodinase, iodothyronine, type II	1.17E-04	1.56	Up	1.09	Down
10886846	Snord113	Small nucleolar RNA SNORD113/SNORD114 family	1.21E-04	1.22	Up	1.52	Down
10902039	RGD1307947/Cep290	Similar to RIKEN cDNA C430008C19/centrosomal protein 290	1.21E-04	1.14	Up	1.33	Down
10907962	Trpc6	Transient receptor potential cation channel, subfamily C, member 6	1.21E-04	1.17	Up	1.30	Up
10735889	rno-mir-22	rno-mir-22 stem-loop	1.25E-04	1.32	Up	1.01	Up
10844992	Lrp1b	Low-density lipoprotein-related protein 1B (deleted in tumors)	1.31E-04	1.28	Up	1.30	Down
10910768	Snord18	Small nucleolar RNA SNORD18	1.33E-04	1.21	Up	1.29	Down
10898474	Pim3	Pim-3 oncogene	1.35E-04	1.24	Up	1.02	Down
10879667	Akirin1	Akirin 1	1.39E-04	1.25	Up	1.02	Down
10847525	Cry2	Cryptochrome 2 (photolyase-like)	1.53E-04	1.24	Up	1.06	Up
10809563	Irx5	Iroquois homeobox 5	1.54E-04	1.38	Down	1.13	Up
10901436	Eid3	EP300 interacting inhibitor of differentiation 3	1.54E-04	1.22	Up	1.18	Down
10795574	Arhgap12	Rho GTPase activating protein 12	1.71E-04	1.14	Up	1.22	Down
10785521	U1	U1 spliceosomal RNA	1.73E-04	1.04	Up	1.43	Down
10938101	Prkx	Protein kinase, X-linked	1.76E-04	1.22	Up	1.12	Down
10900592	Midn	Midnolin	1.78E-04	1.22	Up	1.14	Up
10869010	Zfp189	Zinc finger protein 189	1.80E-04	1.23	Up	1.07	Down
10938995	Itm2a	Integral membrane protein 2A	1.80E-04	1.08	Down	1.25	Down

Table continued

Table 3. *Continued*

Affymetrix transcripts cluster ID	Gene symbol	Gene title	SAM *q* value	FC $t = 0$ h		FC $t = 4$ h	
10716136	Pdcd4	Programmed cell death 4	1.81E-04	1.23	Up	1.37	Down
10868428	Dnajb5	DnaJ (Hsp40) homolog, subfamily B, member 5	1.84E-04	1.24	Up	1.17	Up
10785545	LOC306096	Similar to Dachshund homolog 1 (Dach1)	1.88E-04	1.00	Down	1.29	Up
10762028	Snora67	Small nucleolar RNA SNORA67	1.89E-04	1.31	Up	1.02	Down
10878219	Usp15	Ubiquitin-specific peptidase 15	1.90E-04	1.20	Up	1.28	Down
10803158	Rock1	Rho-associated coiled-coil containing protein kinase 1	2.00E-04	1.14	Up	1.29	Down
10930618	Nd6	nd6	2.08E-04	1.29	Up	1.37	Down
10829896	Atoh7	Atonal homolog 7 (*Drosophila*)	2.11E-04	1.30	Down	1.07	Up
10770334	Mixl1	Mix1 homeobox-like 1 (*Xenopus laevis*)	2.17E-04	1.25	Down	1.13	Up
10778763	Rel	v-rel reticuloendotheliosis viral oncogene homolog (avian)	2.45E-04	1.21	Up	1.04	Down
10906950	LOC100361136	Hypothetical LOC100361136	2.53E-04	1.35	Up	1.08	Down
10884489	G2e3	G2/M-phase specific E3 ubiquitin ligase	2.61E-04	1.36	Up	1.20	Down
10866926	LOC690728	Similar to Protein C12orf11 (sarcoma antigen NY-SAR-95)	2.72E-04	1.21	Up	1.18	Down
10938893	rno-mir-325	rno-mir-325 stem-loop	2.79E-04	1.16	Up	1.45	Down
10896674	Fam91a1	Family with sequence similarity 91, member A1	3.02E-04	1.21	Up	1.21	Down
10863471	Dok1	Docking protein 1	3.07E-04	1.13	Down	1.26	Down
10895861	Ddit3	DNA-damage inducible transcript 3	3.09E-04	1.39	Up	1.07	Up
10791650	Q7TP26_RAT	Q7TP26_RAT	3.16E-04	1.75	Down	1.09	Up
10763421	Dsel	Dermatan sulfate epimerase-like	3.29E-04	1.02	Down	1.46	Down
10840007	Hspa12b	Heat shock protein 12B	3.34E-04	1.35	Down	1.01	Up
10725112	Snord14	Small nucleolar RNA SNORD14	3.38E-04	1.32	Up	1.14	Down
10779681	U1	U1 spliceosomal RNA	3.41E-04	1.44	Up	1.36	Down
10779683	Ktn1	Kinectin 1	3.41E-04	1.12	Up	1.23	Down
10866410	Gpr19	G-protein-coupled receptor 19	3.48E-04	1.23	Up	1.04	Down
10863676	Egr4	Early growth response 4	3.56E-04	1.24	Up	1.27	Up
10934154	Stard8	StAR-related lipid transfer (START) domain containing 8	3.59E-04	1.07	Down	1.21	Up
10929729	Gbx2	Gastrulation brain homeobox 2	3.72E-04	1.28	Down	1.13	Up
10755127	Snora63	Small nucleolar RNA SNORA63	3.78E-04	1.39	Up	1.43	Down
10774681	Smek2	SMEK homolog 2, suppressor of mek1 (*Dictyostelium*)	3.93E-04	1.21	Up	1.18	Down
10929319	Rab18	RAB18, member RAS oncogene family	3.93E-04	1.14	Up	1.36	Down
10705364	Sertad1	SERTA domain containing 1	4.01E-04	1.23	Up	1.14	Down
10792522	Defb10	Defensin β 10	4.07E-04	1.10	Down	1.30	Down
10892912	Cwf19l2	CWF19-like 2, cell cycle control (Schizosaccharomyces *pombe*)	4.08E-04	1.21	Up	1.13	Down
10861560	N5	DNA binding protein N5	4.09E-04	1.42	Up	1.26	Down
10910762	Snord18	Small nucleolar RNA SNORD18	4.26E-04	1.46	Up	1.43	Down
10761128	Hspb1	Heat shock protein 1	4.35E-04	1.46	Up	1.46	Up
10890003	Ppp2r3c	Protein phosphatase 2, regulatory subunit B′′, γ	4.36E-04	1.29	Up	1.20	Down
10915981	Barx2	BARX homeobox 2	4.51E-04	1.17	Down	1.30	Up
10778399	Mospd1	Motile sperm domain containing 1	4.56E-04	1.32	Up	1.14	Down
10746040	U6	U6 spliceosomal RNA	4.64E-04	1.29	Up	1.23	Down
10935021	Armcx5	Armadillo repeat containing, X-linked 5 Gene	4.70E-04	1.26	Up	1.02	Down
10719616	PVR	Poliovirus receptor	4.81E-04	1.23	Up	1.07	Down
10714254	LOC499330	Similar to nicotinamide riboside kinase 1	4.87E-04	1.09	Up	1.44	Down
10869137	Fktn	Fukutin	4.88E-04	1.15	Up	1.27	Down
10797857	Edn1	Endothelin 1	4.96E-04	1.31	Up	1.08	Down
10918535	Fam63b	Family with sequence similarity 63, member B	5.21E-04	1.15	Up	1.28	Down
10722315	U6	U6 spliceosomal RNA	5.22E-04	1.50	Down	1.11	Down
10795344	Q63290_RAT	L1 retroposon, ORF2 mRNA, fragment	5.25E-04	1.31	Down	1.23	Up
10760112	Rnf6	Ring finger protein (C3H2C3 type) 6	5.29E-04	1.10	Up	1.30	Down
10911309	Gtf2a2	General transcription factor IIA, 2	5.45E-04	1.35	Up	1.11	Up
10809766	LOC364956	Hypothetical LOC364956	5.50E-04	1.41	Down	1.04	Up
10899378	Grasp	GRP1 (general receptor for phosphoinositides 1)-associated scaffold protein	5.61E-04	1.23	Up	1.25	Up
10828154	Hspa1	Heat shock protein 1	5.63E-04	1.69	Up	1.04	Up
10844968	Lrp1b	Low-density lipoprotein-related protein 1B (deleted in tumors)	5.70E-04	1.19	Up	1.21	Down
10927717	Kdelc1	KDEL (Lys-Asp-Glu-Leu) containing 1	5.70E-04	1.09	Up	1.20	Down
10748999	Slc25a19	Solute carrier family 25 (mitochondrial thiamine pyrophosphate carrier), member 19	5.89E-04	1.06	Down	1.20	Down
10869644	U6	U6 spliceosomal RNA	6.00E-04	1.42	Down	1.14	Down
10806913	Usp38	Ubiquitin specific peptidase 38	6.09E-04	1.31	Up	1.10	Down
10885600	Cwc22	CWC22 spliceosome-associated protein homolog (*S. cerevisiae*)	6.14E-04	1.19	Up	1.27	Down
10914788	Birc2	Baculoviral IAP repeat-containing 2	6.16E-04	1.25	Up	1.20	Down
10914682	Dync2h1	Dynein cytoplasmic 2 heavy chain 1	6.16E-04	1.11	Up	1.30	Down
10822637	Skil	SKI-like oncogene	6.29E-04	1.24	Up	1.02	Up
10903657	LOC314942	Similar to CUB and Sushi multiple domains 3 isoform 1	6.38E-04	1.06	Up	1.33	Down
10772861	U6	U6 spliceosomal RNA	6.39E-04	1.07	Down	1.44	Down

Table continued

Table 3. *Continued*

Affymetrix transcripts cluster ID	Gene symbol	Gene title	SAM *q* value	FC $t = 0$ h		FC $t = 4$ h	
10775157	LOC689986	Hypothetical protein LOC689986	6.46E-04	1.44	Up	1.03	Up
10799835	Nsun6	NOL1/NOP2/Sun domain family, member 6	6.54E-04	1.25	Up	1.08	Down
10741831	RGD1310862	Similar to adult retina protein	6.68E-04	1.14	Up	1.27	Down
10829163	Snora36	Small nucleolar RNA SNORA36 family	6.68E-04	1.25	Up	1.09	Down
10826547	Mettl14	Methyltransferase like 14	6.95E-04	1.16	Up	1.30	Down
10912525	Stag1	Stromal antigen 1	7.25E-04	1.15	Up	1.21	Down
10795724	Lgals8	Lectin, galactoside-binding, soluble, 8	7.41E-04	1.15	Up	1.26	Down
10802367	Rax	Retina and anterior neural fold homeobox	7.49E-04	1.26	Down	1.23	Up
10788655	Mak16	MAK16 homolog (*S. cerevisiae*)	7.78E-04	1.04	Up	1.27	Down
10912229	Plscr2	Phospholipid scramblase 2	7.86E-04	1.27	Up	1.26	Down
10772072	Uba6	Ubiquitin-like modifier activating enzyme 6	7.87E-04	1.22	Up	1.02	Up
10786995	LOC290577	Hypothetical LOC290577	7.91E-04	1.23	Up	1.17	Down
10889522	Dld	Dihydrolipoamide dehydrogenase	8.04E-04	1.25	Up	1.22	Down
10845070	Snord56	Small nucleolar RNA SNORD56	8.13E-04	1.34	Up	1.21	Down
10772274	Chic2	Cysteine-rich hydrophobic domain 2	8.25E-04	1.14	Up	1.25	Down
10795548	Kif5b	Kinesin family member 5B	8.27E-04	1.15	Up	1.22	Down
10931259	Arl13b	ADP-ribosylation factor-like 13B	8.28E-04	1.15	Up	1.28	Down
10833834	Fxc1	Fractured callus expressed transcript 1	8.29E-04	1.43	Down	1.16	Up
10815778	Lekr1	Leucine, glutamate and lysine rich 1	8.42E-04	1.10	Up	1.26	Down
10798737	Arid4b	AT rich interactive domain 4B (Rbp1 like)	8.49E-04	1.06	Up	1.25	Down
10935589	Htatsf1	HIV-1 Tat specific factor 1	8.51E-04	1.07	Up	1.31	Down
10884853	Prpf39	PRP39 pre-mRNA processing factor 39 homolog (*S. cerevisiae*)	8.57E-04	1.18	Up	1.20	Down
10766880	Mir29b-2	microRNA mir-29b-2	8.58E-04	1.29	Up	1.14	Down
10893368	LOC692116	Similar to RRS1 ribosome biogenesis regulator	8.67E-04	1.09	Down	1.21	Up
10890917	Cwc22	CWC22 spliceosome-associated protein homolog (*S. cerevisiae*)	8.67E-04	1.19	Up	1.25	Down
10798902	Mkx	Mohawk homeobox	8.84E-04	1.16	Up	1.23	Down
10741664	Rpl36a-ps2	Similar to large subunit ribosomal protein L36a	8.84E-04	1.01	Up	1.39	Up
10778620	Slc1a4	Solute carrier family 1 (glutamate/neutral amino acid transporter), member 4	8.86E-04	1.29	Up	1.22	Up
10701709	Lats1	LATS, large tumor suppressor, homolog 1 (*Drosophila*)	8.95E-04	1.07	Up	1.33	Down
10751769	Atp13a3	ATPase type 13A3	8.97E-04	1.14	Up	1.24	Down
10761446	LOC687426	Similar to G-protein-coupled receptor 133	8.97E-04	1.06	Down	1.22	Up
10722521	Mkrn3	Makorin, ring finger protein, 3	9.01E-04	1.20	Down	1.02	Down
10730559	Cuedc2	CUE domain containing 2	9.20E-04	1.24	Up	1.06	Down
10788125	Cdkn2aip	CDKN2A interacting protein	9.35E-04	1.25	Up	1.05	Down
10927871	Stat1/Stat4	Signal transducer and activator of transcription 1/4	9.37E-04	1.02	Down	1.25	Down
10752233	Olr1566	Olfactory receptor 1566	9.42E-04	1.20	Down	1.06	Down
10734258	Grap	GRB2-related adaptor protein	9.52E-04	1.22	Down	1.04	Up
10814858	Atp11b	ATPase, class VI, type 11B	9.53E-04	1.22	Up	1.15	Down
10933408	Mospd2	Motile sperm domain containing 2	9.67E-04	1.23	Up	1.20	Down
10850081	RGD1564425	Similar to proteasome subunit β type 3 (proteasome θ chain)	9.73E-04	1.28	Down	1.16	Up
10712057	Olr292	Olfactory receptor 292	1.00E-03	1.10	Down	1.26	Down
10747202	Krt33b	Keratin 33B	1.01E-03	1.24	Down	1.05	Up
10787017	LOC290577	Hypothetical LOC290577	1.01E-03	1.30	Up	1.19	Down
10772468	Nfxl1	Nuclear transcription factor, X-box binding-like 1	1.01E-03	1.18	Up	1.29	Down
10813347	Ttc33	Tetratricopeptide repeat domain 33	1.01E-03	1.08	Up	1.24	Down
10881063	Clcnka	Chloride channel Ka	1.03E-03	1.21	Down	1.01	Down
10719956	Sdccag1	Serologically defined colon cancer antigen 1	1.04E-03	1.11	Up	1.25	Down
10891659	Rps6ka5	Ribosomal protein S6 kinase, polypeptide 5	1.04E-03	1.12	Up	1.28	Down
10886784	rno-mir-345	rno-mir-345 stem-loop	1.04E-03	1.24	Down	1.02	Down
10765671	Dcaf8	DDB1 and CUL4 associated factor 8	1.05E-03	1.09	Up	1.27	Down
10737426	Tmem100	Transmembrane protein 100	1.05E-03	1.41	Up	1.13	Up
10826403	Snx7	Sorting nexin 7	1.08E-03	1.01	Up	1.20	Up
10783868	Gmpr2/Tinf2	Guanosine monophosphate reductase 2/TERF1 (TRF1)-interacting nuclear factor 2	1.09E-03	1.34	Up	1.00	Up
10917290	Hspb2	Heat shock protein β 2	1.12E-03	1.25	Down	1.07	Up
10756270	5S_rRNA	5S ribosomal RNA	1.13E-03	1.32	Down	1.03	Down
10901367	RGD1309995	Similar to CG13957-PA	1.13E-03	1.11	Up	1.25	Down
10792035	Dusp4	Dual specificity phosphatase 4	1.14E-03	1.35	Up	1.07	Up
10804647	Cdx1	Caudal type homeobox 1	1.15E-03	1.21	Down	1.02	Up
10924076	Rpe	Ribulose-5-phosphate-3-epimerase	1.15E-03	1.00	Up	1.23	Down
10864968	RGD1561270	Similar to zinc finger protein 248	1.15E-03	1.25	Up	1.17	Down
10759435	5S_rRNA	5S ribosomal RNA	1.15E-03	1.32	Down	1.03	Down
10836633	Phospho2	Phosphatase, orphan 2	1.15E-03	1.31	Up	1.06	Down
10833215	Ddx50	DEAD (Asp-Glu-Ala-Asp) box polypeptide 50	1.16E-03	1.25	Up	1.07	Down
10847387	F2	Coagulation factor II (thrombin)	1.17E-03	1.13	Down	1.33	Down

Table continued

Table 3. *Continued*

Affymetrix transcripts cluster ID	Gene symbol	Gene title	SAM *q* value	FC $t = 0$ h		FC $t = 4$ h	
10906428	Abcd2	ATP-binding cassette, subfamily D (ALD), member 2	1.17E-03	1.08	Up	1.23	Down
10939319	Armcx6	Armadillo repeat containing, X-linked 6	1.18E-03	1.04	Up	1.25	Down
10759445	5S_rRNA	5S ribosomal RNA	1.19E-03	1.31	Down	1.04	Down
10756268	5S_rRNA	5S ribosomal RNA	1.20E-03	1.31	Down	1.04	Down
10756272	5S_rRNA	5S ribosomal RNA	1.20E-03	1.32	Down	1.04	Down
10763137	5S_rRNA	5S ribosomal RNA	1.21E-03	1.16	Up	1.25	Down
10737380	Rnft1	Ring finger protein, transmembrane 1	1.21E-03	1.42	Up	1.02	Down
10795289	Hist1h2ail	Histone cluster 1, H2ai-like	1.22E-03	1.34	Down	1.00	Down
10826672	Alpk1	β-Kinase 1	1.23E-03	1.03	Up	1.25	Down
10844988	Lrp1b	Low-density lipoprotein-related protein 1B (deleted in tumors)	1.24E-03	1.31	Up	1.38	Down
10882511	Morn2	MORN repeat containing 2	1.25E-03	1.11	Down	1.27	Down
10875420	LOC502940	Pro-histogranin	1.26E-03	1.21	Down	1.13	Up
10887336	Snora28	Small nucleolar RNA SNORA28	1.27E-03	1.24	Up	1.32	Down
10785865	Abcc4	ATP-binding cassette, subfamily C (CFTR/MRP), member 4	1.28E-03	1.23	Down	1.11	Up
10854303	Cpa4	Carboxypeptidase A4	1.28E-03	1.19	Down	1.21	Down
10936346	Lonrf3	LON peptidase N-terminal domain and ring finger 3	1.31E-03	1.09	Up	1.27	Down
10825580	Hipk1	Homeodomain interacting protein kinase 1	1.34E-03	1.15	Up	1.30	Down
10752654	Znf654	Zinc finger protein 654	1.36E-03	1.25	Up	1.06	Down
10877896	Fam29a	Family with sequence similarity 29, member A	1.40E-03	1.13	Up	1.49	Down
10887966	Hnrpll	Heterogeneous nuclear ribonucleoprotein L-like	1.42E-03	1.22	Up	1.02	Up
10764404	Zbtb41	Zinc finger and BTB domain containing 41	1.42E-03	1.26	Up	1.11	Down
10703327	RGD156237	Similar to chromosome 6 open reading frame 70/LOC361485	1.42E-03	1.13	Up	1.25	Down
10843125	Pcmtd2	Protein-L-isoaspartate (D-aspartate) *O*-methyltransferase domain containing 2	1.43E-03	1.10	Up	1.24	Down
10868669	Zcchc7	Zinc finger, CCHC domain containing 7	1.44E-03	1.04	Up	1.25	Down
10902614	Rap1b	RAP1B, member of RAS oncogene family	1.45E-03	1.22	Up	1.06	Down
10720126	LOC687333	Similar to zinc finger protein 59	1.45E-03	1.26	Up	1.07	Up
10868007	Casp8ap2	Caspase 8 associated protein 2	1.46E-03	1.15	Up	1.25	Down
10764626	Ivns1abp	Influenza virus NS1A binding protein	1.47E-03	1.22	Up	1.01	Down
10901039	LOC100364912	rCG29233-like	1.50E-03	1.21	Up	1.05	Down
10815442	Spg20	Spastic paraplegia 20 (Troyer syndrome) homolog (human)	1.50E-03	1.11	Up	1.25	Down
10850492	RGD1308023	Similar to CG5521-PA	1.51E-03	1.15	Up	1.24	Down
10850958	Pxmp4	Peroxisomal membrane protein 4	1.56E-03	1.21	Down	1.06	Down

Shown are the Affymetrix transcripts cluster ID, gene symbol, gene title, SAM *q* value, and fold change at $t = 0$ h and $t = 4$ h, together with the direction of regulation (up or down), of the differentially expressed genes obtained by microarray analysis in the barrel cortex after enriched environment. Genes are ordered by significance (most significant genes on top). Only well-annotated genes are included.

solution (30% ethyleneglycol, 20% glycerol in sodium phosphate buffer, pH 7.3) until additional analysis.

RNA isolation. Tissue samples were homogenized with a TissueLyser (Retsch GmbH) in TRIzol Reagent (Invitrogen), according to the protocol of the manufacturers. The procedure was modified for small amounts of tissue by using 800 μl of TRIzol Reagent and adding 1 μl of glycogen (Fermentas). RNA concentration and quality was determined with a NanodropTM ND-1000 spectrophotometer (Thermo Fisher Scientific) and 1% agarose gel electrophoresis, respectively. The samples were kept at −80°C until additional analysis.

Microarray analysis. Samples from UNCLIP groups (with and without EE) were processed for microarray analysis. To reduce variability, RNA samples were pooled (three samples per pool), resulting in 12 pools (two to four pools per experimental group). The pooled samples were purified with the NucleoSpin RNA II kit (Macherey-Nagel GmbH & Co.) and sent to ServiceXS BV for additional processing. Sample concentration and integrity was checked with a Bioanalyzer 2100 (Agilent Technologies), followed by labeling using the Affymetrix Transcript (WT) Single-Stranded Target Labeling kit, hybridization to the GeneChip Rat Gene 1.0 ST Array (both from Affymetrix), and scanning. The Affymetrix Command Console and Expression Console software were used for the performance of the washing, staining, and scanning of the chips. Data quality controls were within Affymetrix specifications.

Normalization of the microarray data was performed with GeneSpring GX version 11 (Agilent Technologies). The raw data were summarized using ExonRMA as a summarization algorithm, followed by log and baseline transformation to the median of all the samples. After transformation, data were filtered on expression (20–100th percentile). Normalized data were analyzed by Significance Analysis of Microarrays (SAM) as described previously (Tusher et al., 2001), using the "samr" package (http://www-stat.stanford.edu/~tibs/SAM) in R version 2.12.0 (http://www.r-project.org). Criteria for differential expression were a p value ≤ 0.05 (delta 2.05) and a fold change (FC) $\geq |1.2|$. Gene ontology (GO) enrichment analysis of the differentially expressed genes was performed using the Web-based gene ontology tool from the Database for Annotation, Visualization, and Integrated Discovery (DAVID) version 6.7 (http://david.abcc.ncifcrf.gov) (Dennis et al., 2003; Huang et al., 2009). This analysis was performed by using the Functional Annotation Chart (in which GO enrichment in the list of differentially expressed genes is tested) and the Functional Annotation Clustering tool (which groups redundant GO terms in clusters to facilitate the interpretation of the results). For the enrichment analysis (Functional Annotation Chart tool), default software settings were used, and GO terms with a p value [or EASE score (for Expression Analysis Systematic Explorer)] ≤ 0.05 were considered to be overrepresented (enriched). For the Functional Annotation Clustering tool, the classification stringency was set as high, and only clusters with an enrichment score ≥ 1.3 (equivalent to non-log scale p of 0.05) were considered.

Quantitative PCR. Before cDNA synthesis, 2 μg of each RNA sample was treated with 2 U of DNase (Fermentas) in the presence of RiboLock RNase Inhibitor (20 U/μl) (Fermentas). For cDNA synthesis, through random priming, the RevertAid H Minus First Strand cDNA Synthesis kit (Fermentas) was used, following the guidelines of the manufacturer. Before analysis, 15 μl of each cDNA sample was diluted with 185 μl of MilliQ water. qPCR reactions were performed with the Rotor-Gene 6000 Series (Corbett Life Science Pty. Ltd.). For each reaction, 2.5 μl of each diluted sample of cDNA was added to a mix containing 6.25 μl of 2× Maxima SYBR Green qPCR Master Mix (Fermentas), 1 μl of each primer (5 μM), and 1.75 μl of MilliQ water. Primers were designed using NCBI Primer-Blast (www.ncbi.nlm.nih.gov/tools/primer-blast/) and synthe-

Table 4. Functional clusters of enriched GO categories (most significant category of each cluster shown)

Annotation cluster #	Term	Category	Count	Genes	*p* value	Fold enrichment	Enrichment score
1	Transcription	GOTERM_BP_FAT	29	Per1, Ddit3, Egr2, Jun, Arid4b, Klf2, Nr4a3, Eid3, Ccnl1, Rax, Med14, Egr4, Txnip, Nr4a2, Nfil3, Fos, JunB, Npas4, Nr4a1, Btg2, Egr3, Zbtb10, Cry2, Gtf2a2, Crem, Stat1/Stat4, Atf3, FosB, Egr1	9.08E-09	3.49	7.0
2	Positive regulation of macromolecule metabolic process	GOTERM_BP_FAT	28	Ddit3, Csrnp1, Klf4, Egr2, Zfp36, Rnf6, Jun, Irs2, F2, Klf2, Nr4a3, Hnrpll, Med14, Egr4, Barx2, Cdx1, Nr4a2, Rel, Gmpr2/Tinf, Klf4, Fos, JunB, Npas4, Nr4a1, Inhba, Gtf2a2, Pdgfb, Sertad1, Egr1	2.23E-06	2.74	5.9
3	Basic-leucine zipper (bZIP) transcription factor	INTERPRO	8	Ddit3, Crem, Jun, FosB, Atf3, JunB, Fos, Nfil3	1.34E-06	13.89	5.1
4	Regulation of apoptosis	GOTERM_BP_FAT	21	Sgk1, Txnip, Ddit3, Hipk1, Nr4a2, Rel, Jun, Rock1, Casp8ap2, Nr4a1, Btg2, Bdnf, Skil, Inhba, Dusp1, Hspb1, G2e3, Hspa1a/Hspa1l/Hspa1b, Ptgs2, Birc2, Stat1/Stat4	1.64E-04	2.56	3.7
5	Membrane-enclosed lumen	GOTERM_CC_FAT	27	Klf4, Rnf6, Jun, Dld, Ptgs2, Ccnl1, Med14, Barx2, Txnip, Dusp6, Zbtb33, Hipk1, Dusp4, Rps6ka5, Rel, Midn, Gmpr2/Tinf, Klf4, Fos, Npas4, Nr4a1, Cdkn2aip, Gtf2a2, Pdgfb, Fxc1-ps1/Fxc1, Crem, Stat1/Stat4, Atf3	1.90E-04	2.13	3.3
6	Negative regulation of cellular biosynthetic process	GOTERM_BP_FAT	18	Per1, Barx2, Txnip, Klf4, Dnajb5, Gmpr2/Tinf, Sik1, Klf4, Kdm6b, Insig1/LOC688922, Skil, Foxn3, Bcl6b, Zbtb10, Pdgfb, Pdcd4, Edn1, Egr1, Hbegf	9.11E-05	3.00	2.9
7	Response to oxidative stress	GOTERM_BP_FAT	8	Nd6, Txnip, Ddit3, Dusp1, Ptgs2, Jun, Stat1/Stat4, Fos	6.38E-03	3.63	2.7
8	Regulation of synaptic transmission	GOTERM_BP_FAT	8	Plk3, Bdnf, Plat, Arc, Egr2, Ptgs2, Edn1, Egr1	3.68E-03	4.02	2.6
9	Transcription from RNA polymerase II promoter	GOTERM_BP_FAT	7	Med14, Ddit3, Gtf2a2, Jun, FosB, JunB, Fos	1.10E-03	5.95	2.4
10	Phosphate metabolic process	GOTERM_BP_FAT	20	Sgk1, Dusp6, Dusp4, Pim3, Gpd1, Rps6ka5, Alpk1, Sik1, Rock1, Fam63b, Dld, Bdnf, Plk3, Gadd45b, Gadd45g, Dusp1, Prkx, Lats1, Stat1/Stat4, Trib1	4.08E-03	2.02	2.2
11	Blood vessel morphogenesis	GOTERM_BP_FAT	8	Gbx2, Plat, Cyr61, Tiparp, Jun, Edn1, JunB, Apold1	6.98E-03	3.57	1.8
12	Negative regulation of protein kinase activity	GOTERM_BP_FAT	6	Dusp6, Gadd45g, Gadd45b, Hmgcr, Pdcd4, Trib1	1.64E-03	6.94	1.7
13	Positive regulation of apoptosis	GOTERM_BP_FAT	10	Nr4a1, Txnip, Inhba, Ddit3, Dusp1, Hipk1, Ptgs2, Jun, Stat1/Stat4, Casp8ap2	1.91E-02	2.48	1.7
14	Zinc finger, C2H2-type/integrase, DNA-binding	INTERPRO	6	Egr4, Egr3, Zbtb10, Egr2, Klf2, Egr1	4.49E-02	3.07	1.7
15	Response to bacterium	GOTERM_BP_FAT	7	Defb10, Ptgs2, Jun, Stat1/Stat4, Fos, Pcsk1, Trib1	4.62E-02	2.67	1.6
16	Response to progesterone stimulus	GOTERM_BP_FAT	4	Txnip, FosB, JunB, Fos	6.56E-03	10.30	1.6
17	ATPase activity, coupled to transmembrane movement of substances	GOTERM_MF_FAT	5	Abcc4, Atp11b, Atp13a3/LOC678704, Abcg2, Abcb1a	3.19E-02	4.15	1.6
18	Dual specificity protein phosphatase (MAP kinase phosphatase)	PIR_SUPERFAMILY	3	Dusp6, Dusp1, Dusp4	1.83E-03	42.71	1.4
19	ABC transporters	KEGG_PATHWAY	4	Abcc4, Abcd2, Abcg2, Abcb1a	8.77E-03	9.14	1.4
20	Nerve growth factor IB-like nuclear receptor	PIR_SUPERFAMILY	3	Nr4a1, Nr4a2, Nr4a3	5.58E-04	71.18	1.3
21	Sterol biosynthetic process	GOTERM_BP_FAT	4	Insig1/LOC688922, Idi1, Hmgcr, Ch25 h	5.98E-03	10.64	1.3
22	Negative regulation of apoptosis	GOTERM_BP_FAT	9	Btg2, Sgk1, Bdnf, Hspb1, Nr4a2, G2e3, Hspa1a/Hspa1l/Hspa1b, Birc2, Rock1	4.99E-02	2.21	1.3
23	Nucleotide binding	GOTERM_MF_FAT	34	Htatsf1, Abcc4, Sgk1, Rap1b, Atp11b, Hmgcr, Abcg2, Rock1, Ddx50, Dld, Plk3, LOC306096, Hspa1a/Hspa1l/Hspa1b, Atp13a3/LOC678704, Lats1, Arl5b, Hnrpll, Abcb1a, Trib1, Pim3, Gpd1, Rps6ka5, Kif5b, Arl4d, Arl13b, Alpk1, Sik1, Mat2a, LOC499330, Prkx, Mat2a, Abcd2, Cry2, Rab18, Dync2h1	1.81E-02	1.47	1.3

Shown are the different functional clusters of significantly enriched GO categories of the differentially expressed genes. For each cluster, the term, category, count, and genes (Gene symbol) are shown, together with the *p* value and the fold enrichment.

sized at Biolegio BV. Primer sequences are listed in Table 1. Cycling conditions were 10 min 95°C, followed by 40 cycles of 15 s at 95°C, 30 s at 60°C, and 30 s at 72°C. After cycling, a melting protocol was performed, from 72°C to 95°C, measuring fluorescence every 1°C, to control for product specificity.

Relative expression of the genes of interest was calculated after obtaining the corresponding Ct values and correcting for unequal sample input using geNorm (Vandesompele et al., 2002), which identifies the two most stably expressed housekeeping genes (*Ywhaz* and *CycA*) from a set of three tested candidate genes reported previously to be stably expressed in the brain (Bonefeld et al., 2008) to calculate a normalization factor for each sample. This normalization factor was then used to obtain the relative differences between the samples for each primer pair. Statistics were performed using SPSS 17.0 (SPSS Inc.). Normalized data were tested

Table 5. Significantly overrepresented pathways

Pathway #	Term	Category	Count	Genes	*p* value	Fold enrichment
1	MAPK signaling pathway	KEGG_PATHWAY	16	Rap1b, Dusp6, Ddit3, Dusp4, Rps6ka5, Jun, Fos, Nr4a1, Bdnf, Hspb1, Gadd45g, Dusp1, Gadd45b, Prkx, Hspa1l, Pdgfb	2.20E-08	5.98
2	Platelet-derived growth factor receptor signaling pathway	GOTERM_BP_FAT	5	Txnip, Plat, Csrnp1, Tiparp, Pdgfb	1.41E-04	18.14
3	Enzyme linked receptor protein signaling pathway	GOTERM_BP_FAT	12	Txnip, Skil, Plat, Csrnp1, Tiparp, Pdgfb, Jun, Tob1, Fos, Dok1, Irs2, Hbegf	5.43E-04	3.55
4	Transmembrane receptor protein tyrosine kinase signaling pathway	GOTERM_BP_FAT	8	Txnip, Plat, Csrnp1, Tiparp, Pdgfb, Dok1, Irs2, Hbegf	8.31E-03	3.45
5	Transmembrane receptor protein serine/threonine kinase signaling pathway	GOTERM_BP_FAT	5	Skil, Pdgfb, Jun, Tob1, Fos	1.82E-02	4.93
6	Transforming growth factor β receptor signaling pathway	GOTERM_BP_FAT	4	Skil, Pdgfb, Jun, Fos	1.83E-02	7.10
7	Neurotrophin signaling pathway	KEGG_PATHWAY	5	Rap1b, Bdnf, Rps6ka5, Jun, Irs2	3.63E-02	3.90

Shown are the pathways that were overrepresented from the GO analysis of the differentially expressed genes. For each pathway, the term, category, count, and genes (Gene symbol) are shown, together with the *p* value and the Fold enrichment.

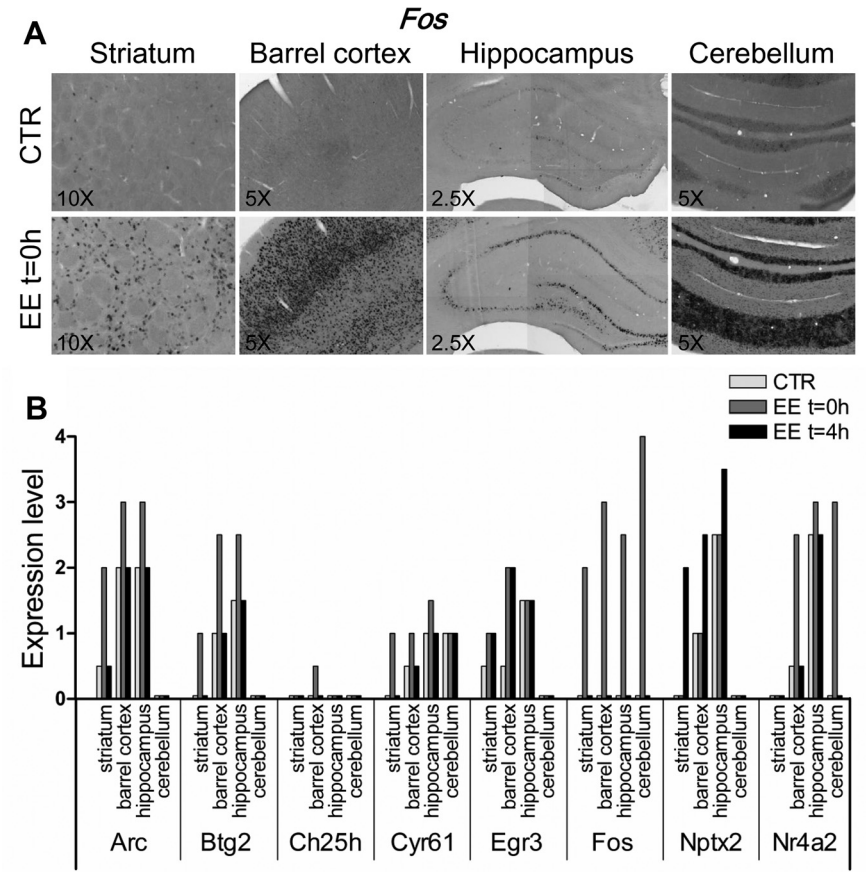

Figure 2. Representative brain areas activated by enrichment. ***A***, Shown are representative images of *Fos* mRNA obtained by *in situ* hybridization in CTR and EE animals at $t = 0$ h. In CTR animals, Fos levels were barely detectable, whereas in EE animals, increased levels were observed in striatum, barrel cortex, hippocampus, and cerebellum. Magnifications are shown at the bottom left corner on each image. ***B***, Expression levels of the eight genes (*Arc*, *Btg2*, *Ch25h*, *Cyr61*, *Egr3*, *Fos*, *Nptx2*, and *Nr4a2*) selected for *in situ* hybridization were quantified in CLIP animals in the four above-mentioned brain areas, showing different regional and temporal patterns of expression under CTR and EE conditions.

for variance homogeneity using Levene's test, and, in case of non-homogeneous data, a log transformation was applied. To directly compare the values (FC) obtained by microarray and qPCR analysis, a two-tailed Pearson's correlation was used. In addition, to compare expression levels between the different groups, univariate two-way ANOVAs were performed separately for each gene in the UNCLIP and CLIP groups, followed, when appropriate, by SNK *post hoc* analyses and independent samples *t* tests, with a significance level of $p \leq 0.05$. To estimate the specificity of the changes in gene expression, we calculated a "specificity index" for each time point, defined as the ratio *A*/*B*, with *A* being the difference in individual EE expression levels and average CTR expression levels in the spared [right (R)] cortical side (individual EE R − average CTR R) and *B* being the difference in individual EE expression levels and average CTR expression levels in the deprived [left (L)] cortical side (individual EE L − average CTR L). This ratio was used to test with a one-sample *t* test (test value 1, significance level $p \leq 0.05$) whether expression levels in the spared (R) side were higher than in the deprived (L) side.

In situ *hybridization.* The plasmid containing the full-length rat activity-regulated cytoskeleton-associated protein (*Arc*) cDNA subcloned into the EcoRI–XhoI site of pBluescriptII SK+ (Stratagene) was kindly provided by Dr P. F. Worley (John Hopkins University, Baltimore, MD). The plasmid was linearized with EcoRI or XhoI and transcribed with T7 or SP6 RNA polymerases to generate antisense and sense probes, respectively. For the other genes, nested PCR was used to obtain DNA templates for sense and antisense probe generation of the gene of interest. Primers were designed using NCBI Primer-Blast (www.ncbi.nlm.nih.gov/tools/primer-blast/) and synthesized at Biolegio BV, adding T3 (5′AATTAACCCTCACTAAAGGG3′) and T7 (5′TAATACGACTCACTATAGGG3′) RNA polymerase sequences at the 5′ end of the forward and reverse internal primers, respectively (primer sequences are listed in Table 2). For the first (external) run, 3 μl of cDNA was mixed with 1.6 μl of each external primer (5 μM), 2 μl of 10× PCR buffer, 0.2 μl of dNTP mix, 0.1 μl of Taq polymerase, and 11.5 μl of DEPC water to a final volume of 20 μl (all from Fermentas). The same components were used for the internal reaction, using a 1:100 dilution of the external run end product as a template and the internal primers. A touchdown protocol was used for both runs. To activate the enzyme, the mix was heated to 94°C for 2 min (hot start), followed by 10 cycles of 60 s at 94°C, 30 s at 68°C (−1°C per cycle), and 90 s at 72°C. Subsequently, 30 cycles were added of 60 s at 94°C, 30 s at 58°C, and 90 s at 72°C, with a final step of 10 min at 72°C. After the PCR reaction, the samples were separated on a 1% agarose gel, and the correct products were gel extracted using the QIAEX II

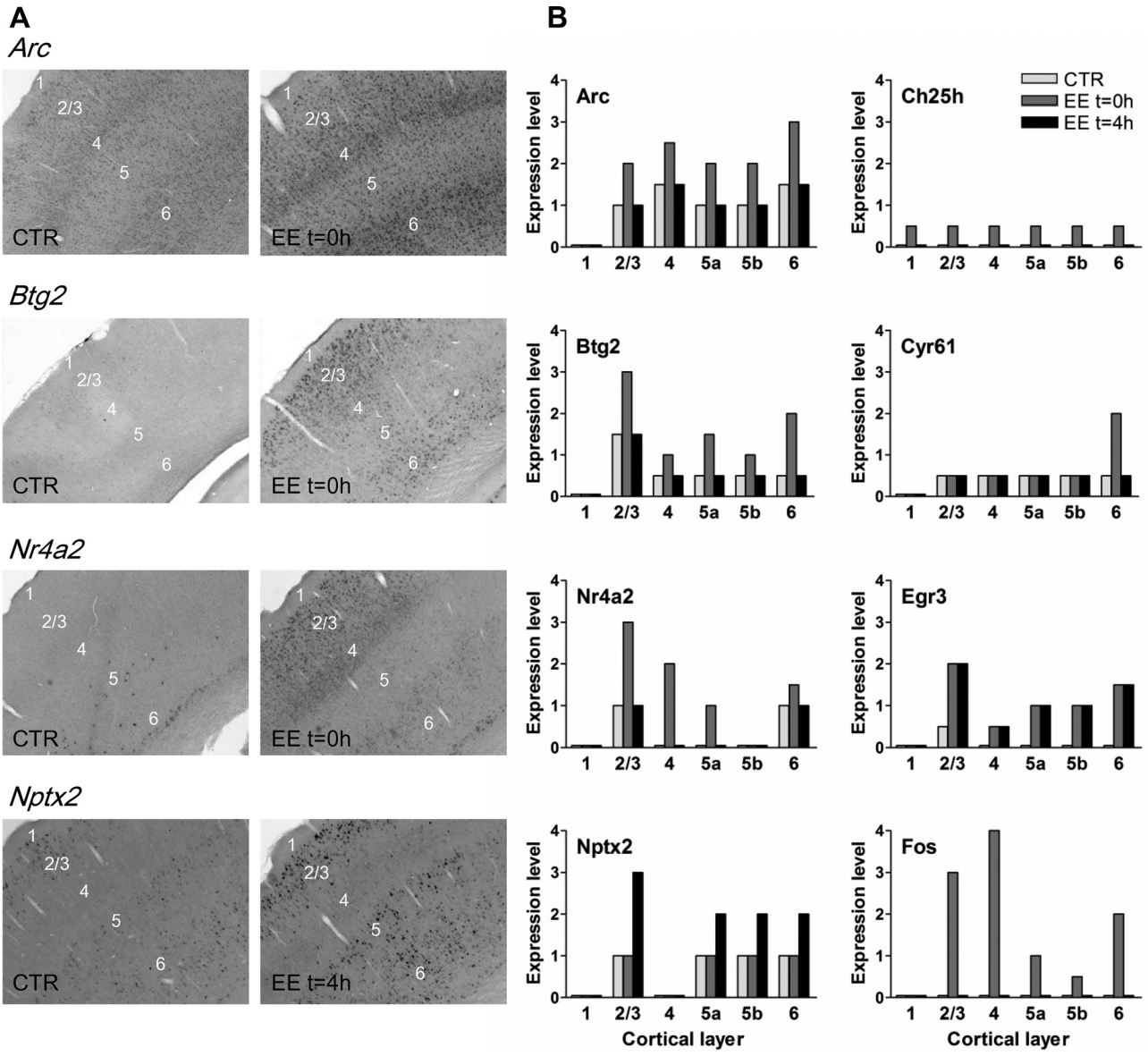

Figure 3. Layer-specific differential gene expression in rat barrel cortex after EE. ***A***, Representative images of *in situ* hybridization analysis of *Arc*, *Btg2*, *Nr4a2*, and *Nptx2* mRNA in UNCLIP groups: CTR and EE animals at $t = 0$ h (*Arc*, *Btg2*, *Nr4a2*) or $t = 4$ h (*Nptx2*); cortical layers are indicated on each image (magnification, 5×). ***B***, Quantification of *Arc*, *Btg2*, *Nr4a2*, *Nptx2*, *Ch25h*, *Cyr61*, *Egr3*, and *Fos* expression levels (*in situ* hybridization) in different cortical layers of UNCLIP animals, under CTR, EE $t = 0$ h, and EE $t = 4$ h conditions.

kit (Qiagen Benelux BV), measuring their concentration with a Nanodrop ND-1000 spectrophotometer (Thermo Fisher Scientific).

Sense and antisense digoxigenin (DIG)-labeled probes were generated by *in vitro* transcription using SP6, T3, or T7 RNA polymerases, depending on the probe. The 20 μl of mixture included 0.3–1 μg of probe template, 1 mM each of ATP, CTP, and GTP, 0.7 mM UTP, 0.3 mM DIG–UTP (Roche Applied Science), 40 U of RiboLock RNase inhibitor, 1× transcription buffer, and 40 U of SP6, T7, or T3 RNA polymerase (all from Fermentas). After 2 h incubation at 37°C, the probe template was digested with 2 U of RNase-free DNase I (Fermentas) for 15 min at 37°C. The labeled cRNA probe was then precipitated overnight by adding 1 μl of glycogen (Fermentas), 2.5 μl of 4 M LiCl, and 75 μl 100% ethanol and recovered by centrifuging at 4°C for 15 min. The pellet was washed twice and resuspended in 25 μl of DEPC H_2O. The amount of labeled probe was quantified by spot blot using DIG-labeled control RNA of known concentration (Roche Applied Science) for comparison. The resulting DIG-labeled probes were stored in nuclease free water at −20°C.

In situ hybridization was performed in free-floating tissue sections using DIG-labeled riboprobes as described previously (Schaeren-

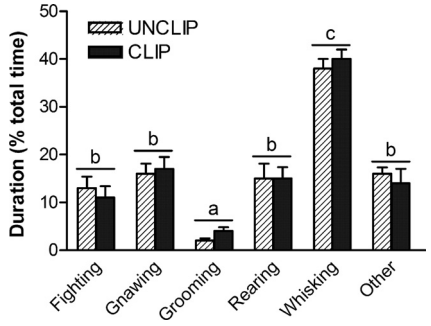

Figure 4. Behavioral analysis of UNCLIP and CLIP animals during exposure to EE. Shown is the amount of time that the animals displayed a certain behavior (namely, fighting, gnawing, grooming, rearing, whisking, and other behaviors). The measurements were performed during a period of 10 min, starting 10 min after the beginning of the EE exposure, in both UNCLIP and CLIP animals (white and gray bars, respectively). Bars represent average ± SEM ($n = 6–8$). Homogeneous subsets are indicated with the same characters (***a–c***) above the bars (two-way ANOVA, $p \leq 0.001$; *post hoc* SNK test).

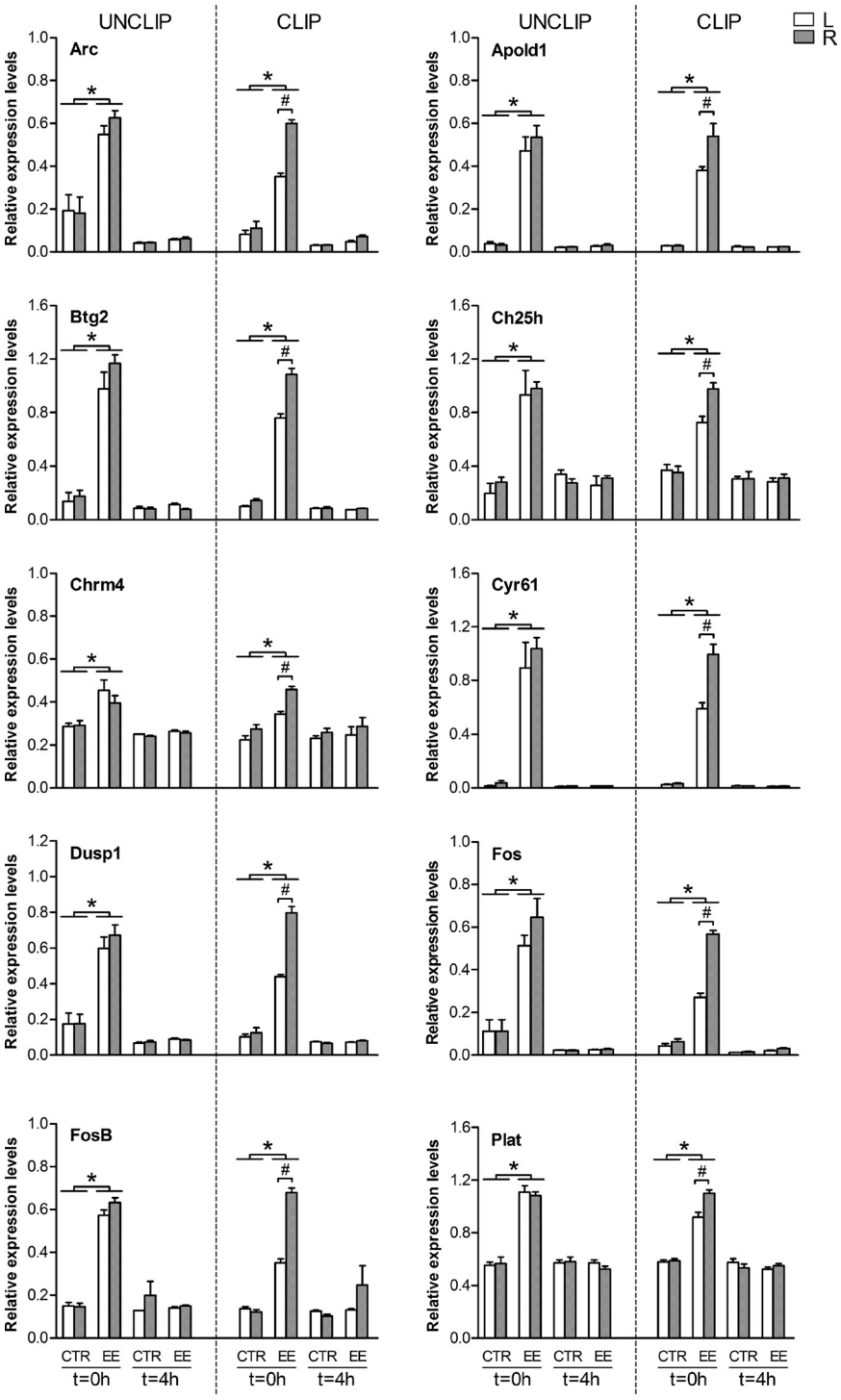

Figure 5. qPCR analysis of gene expression in the rat barrel cortex after EE. Normalized expression values of *Arc*, *Apold1*, *Btg2*, *Ch25h*, *Chrm4*, *Cyr61*, *Dusp1*, *Fos*, *FosB*, and *Plat* mRNA at $t = 0$ h and $t = 4$ h after exposure to EE for 30 min, in UNCLIP (right group of bars) and CLIP (left group of bars) animals. For normalization, *CycA* and *Ywhaz* were selected as housekeeping genes. Measurements were made separately for left (L, white bars) and right (R, gray bars) barrel cortices. Note that, in CLIP groups, L barrel cortex is deprived of sensory input attributable to unilateral clipping of the right whiskers. Bars represent average normalized expression values ± SEM. * represents significant differences between CTR and EE groups (two-way ANOVA, $p \leq 0.05$; *post hoc* SNK test). # represents significant differences between L and R barrel cortices within the same group and time point ($p \leq 0.05$, Student's *t* test). In the deprived (L) barrel cortex of CLIP animals, for all analyzed genes, expression levels were significantly higher in EE than in CTR groups at $t = 0$ h, indicative of residual activation in the deprived cortex ($p \leq 0.05$, Student's *t* test); for the sake of clarity, these significant differences have not been marked by a symbol in the figure.

Wiemers and Gerfin-Moser, 1993; Korosi et al., 2006), with minor modifications. All the steps were performed under RNase-free conditions and at room temperature unless stated otherwise. Throughout the procedure, the sections were kept under gentle agitation in six-well plates using Netwells (both from Corning Inc.). Briefly, sections were washed in PBS followed by a 30 min postfixation with 4% PFA in 0.1 M Borax. Next, sections were permeabilized with 0.2 M HCl, washed in PBS, and treated with 0.01 mg/ml proteinase K (Roche Applied Science) in 0.1 M Tris, 0.05 M EDTA buffer, pH 8.0, for 15 min at 37°C. The sections were acetylated with 0.1 M TEA containing 0.25% acetic anhydride (Sigma-Aldrich), followed by overnight incubation at 58°C in hybridization buffer [50% deionized formamide (Ambion), 1× Denhardt's solution and 10% dextran sulfate (both from Sigma-Aldrich), 0.5 mg/ml tRNA (Roche Applied Science), 0.3 M NaCl, 1 mM EDTA, and 10 mM Tris, pH 8.0] containing 1 ng/ml of the DIG-labeled probe. The next day, sections were washed in 4× SSC and treated with 0.01 mg/ml RNase A (Sigma-Aldrich) in 0.5 M NaCl, 0.01 M Tris, and 1 mM EDTA buffer, pH 8.0, for 15 min at 37°C for 30 min at 37°C, followed by washing steps in decreasing concentrations of SSC, including a 30 min wash in 0.1× SSC at 58°C, several rinses in TBS, and 1 h blocking [0.05% blocking reagent (Roche Applied Science) in TBS]. Sections were then incubated for 3 h with sheep anti-DIG–AP (1:5000; Roche Applied Science), followed by several rinses in alkaline phosphatase (AP) buffer (50 mM $MgCl_2$ in TBS, pH 9.5) and overnight incubation with nitroblue-tetrazolium-chloride/5-bromo-4-chlor-indolyl-phosphate (NBT/BCIP) medium [175 μl NBT/BCIP stock solution (Roche Applied Science) in 10 ml of AP buffer, containing 0.24 mg/ml levamisole] in the dark. Staining was stopped by several washes in 0.1 M Tris, 0.01 M EDTA buffer, pH 8.0, and sections were mounted on Superfrost Plus slides (Thermo Fisher Scientific), air dried, dehydrated in increasing ethanol concentrations, fixed briefly with isopropanol and acetone, cleared in xylene, and coverslipped with Entellan (Merck Chemicals). The sections were examined under a Leica DM 6000B microscope and representative pictures captured with a Leica DFC480 CCD camera using Leica IM500 imaging software (Leica Microsystems). In addition, a qualitative analysis was performed by a blind observer to determine expression levels, ranked as undetectable (0), low (1), medium (2), high (3), and very high (4), in various brain regions (striatum, cortex, hippocampus, and cerebellum) and in the different cortical layers.

Results

Microarray analysis reveals differentially expressed genes in rat barrel cortex after *in vivo* somatosensory experience

To study experience-dependent changes in mRNA expression at the level of the

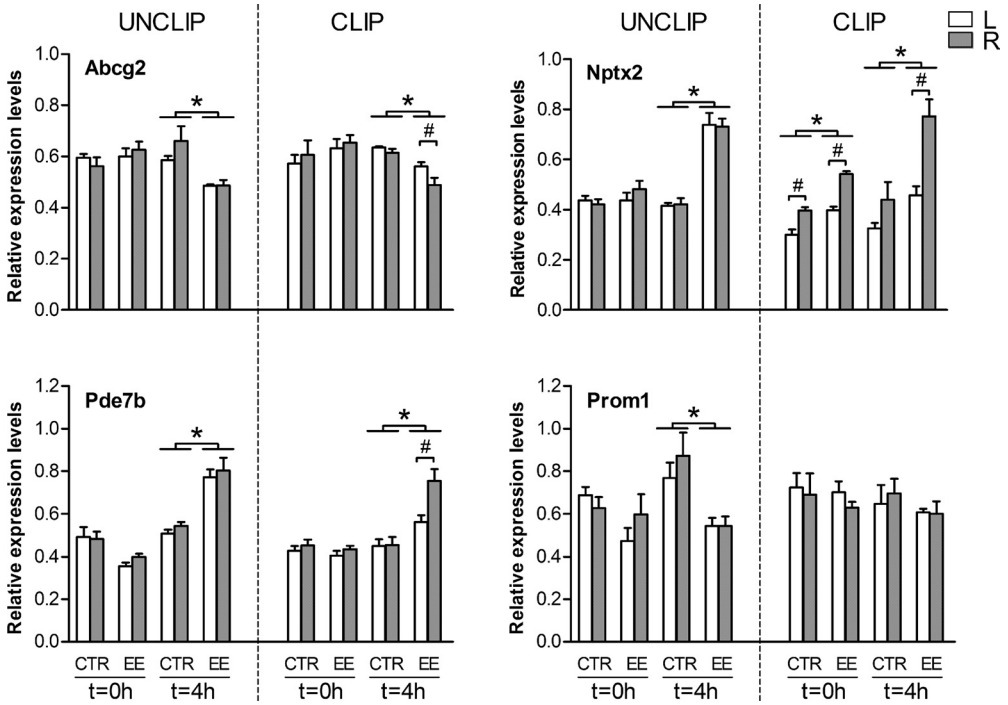

Figure 6. qPCR analysis of gene expression in the rat barrel cortex after EE. Normalized expression values of *Abcg2*, *Nptx2*, *Pde7b*, and *Prom1* mRNA in rat somatosensory cortex at $t = 0$ h and $t = 4$ h after exposure to EE for 30 min, in UNCLIP (right group of bars) and CLIP (left group of bars) animals. For normalization, *CycA* and *Ywhaz* were selected as housekeeping genes. Measurements were made separately for left (L, white bars) and right (R, gray bars) barrel cortices. Note that, in CLIP groups, L barrel cortex is deprived of sensory input attributable to unilateral clipping of the right whiskers. Bars represent average normalized expression values ± SEM. * represents significant differences between CTR and EE groups (two-way ANOVA, $p \leq 0.05$; *post hoc* SNK test). # represents significant differences between left and right barrel cortices within the same group and time point ($p \leq 0.05$, Student's *t* test). In the deprived (L) barrel cortex of CLIP animals, for all analyzed genes, expression levels were significantly higher in EE than in CTR groups at $t = 4$ h, except for *Prom1*, indicative of residual activation in the deprived cortex ($p \leq 0.05$, Student's *t* test); for the sake of clarity, these significant differences have not been marked by a symbol in the figure.

barrel cortex, adult rats were placed in the dark, per two, in an enriched cage during a short (30 min) period. The animals had been habituated previously to the empty test cages to minimize stress-induced artifacts. In contrast to caged-control (CTR) animals, EE exposure induced strong exploratory behavior, especially through active whisking. Importantly, stress-induced behaviors such as self-grooming (Spruijt et al., 1992) were hardly observed, indicating that the habituation procedure successfully reduced novelty-associated stress.

To determine which genes were differentially expressed in the barrel cortex after EE, mRNA expression profiling was performed using microarrays. Expression levels were determined at two time points after the EE session, namely 0 and 4 h, and compared with those observed in CTR rats. Significant differences in gene expression were observed at both time points after EE compared with the respective CTR groups, with 170 genes upregulated and 31 downregulated at $t = 0$ h and 29 upregulated and 98 downregulated genes at $t = 4$ h (Table 3). Of all the differentially expressed genes, 40 were identified at both time points after EE.

Validation of microarray results by qPCR analysis

To validate our results, we verified the differential expression of a subset of genes by qPCR analysis. The genes were selected on the basis of their functional annotation (a wide range of biological functions was chosen, including transcription factor activity, nuclear receptors, cholesterol metabolism, and regulation of synaptic plasticity). A total of 18 genes, ranging from low to high FC and *p* values, were selected for validation, together with three housekeeping gene candidates for normalization (for a list of selected genes and primer pairs, see Table 1). To estimate the validation rate, the normalized expression levels obtained by qPCR (normalized against *CycA* and *Rywhaz* as the two most stable housekeeping genes) were used to calculate an FC for each time point, similar to the microarray analysis (i.e., EE vs CTR at $t = 0$ h and $t = 4$ h). The FCs obtained by the microarray and qPCR analyses were highly correlated (Pearson's correlation, two-tailed, $r^2 = 0.992$, $p \leq 0.0001$ at $t = 0$ h and $r^2 = 0.927$, $p \leq 0.001$ at $t = 4$ h), strongly supporting the validity of the criteria used for the microarray data analysis. In summary, these results show that the expression of a number of genes is modified by increased sensory exploration in the rat barrel cortex, the majority of genes being upregulated at $t = 0$ h and downregulated at $t = 4$ h.

Overrepresented GO categories of the differentially expressed genes

The observed massive EE-induced regulation of gene expression in the barrel cortex suggests that a short but intense period of sensory experience is able to trigger major cellular changes, which could potentially lead to changes in neuronal circuits. To classify these changes, we used a GO enrichment and functional clustering analysis [DAVID version 6.7 (Dennis et al., 2003; Huang et al., 2009)] as a tool to test whether particular functional categories were overrepresented (enriched) in our dataset. From the list of differentially expressed genes (both at $t = 0$ h and $t = 4$ h), as much as 249 significantly overrepresented GO terms were identified, using as a background list all genes present on the array (modified Fisher's exact test, EASE score ≤ 0.05). These GO terms were grouped into 23 functional clusters (DAVID Fuzzy clustering, enrichment score ≥ 1.3), including regulation of cel-

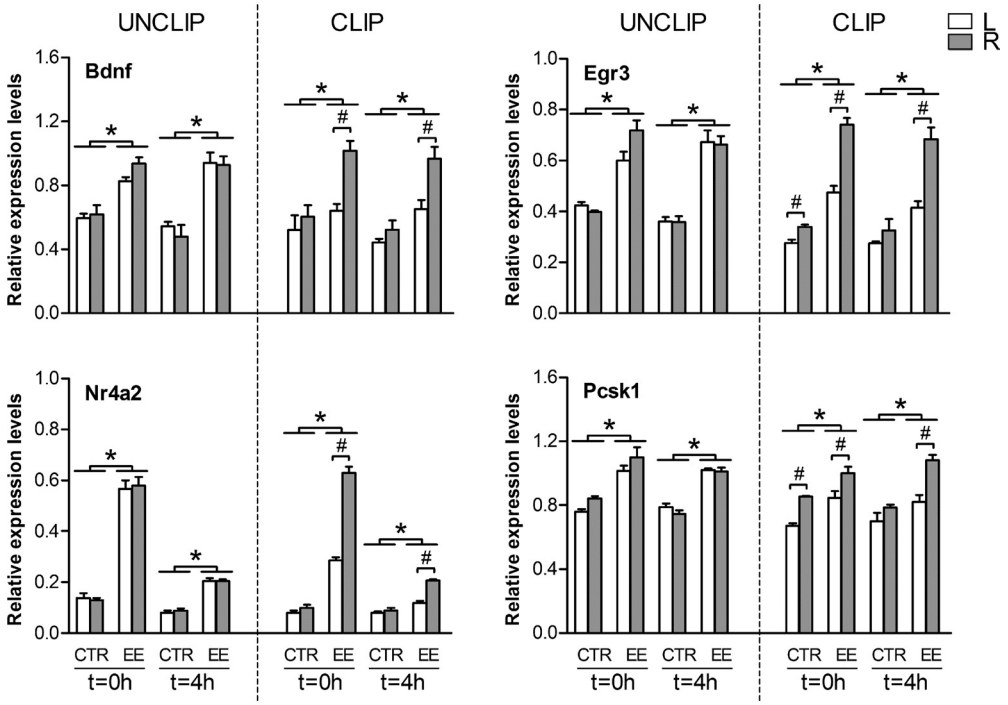

Figure 7. qPCR analysis of gene expression in the rat barrel cortex after EE. Normalized expression values of *Bdnf*, *Egr3*, *Nr4a2*, and *Pcsk1* mRNA in rat somatosensory cortex at $t = 0$ h and $t = 4$ h after exposure to EE for 30 min, in UNCLIP (right group of bars) and CLIP (left group of bars) animals. For normalization, *CycA* and *Ywhaz* were selected as housekeeping genes. Measurements were made separately for left (L, white bars) and right (R, gray bars) barrel cortices. Note that, in CLIP groups, L barrel cortex is deprived of sensory input attributable to unilateral clipping of the right whiskers. Bars represent average normalized expression values ± SEM. * represents significant differences between CTR and EE groups (two-way ANOVA, $p \leq 0.05$; *post hoc* SNK test). # represents significant differences between left and right barrel cortices within the same group and time point ($p \leq 0.05$, Student's *t* test). In the deprived (L) barrel cortex of CLIP animals, for all analyzed genes, expression levels were significantly higher in EE than in CTR groups at $t = 0$ h and $t = 4$ h, except for *Bdnf* at $t = 0$ h and *Pcsk1* at $t = 4$ h, indicative of some activation in the deprived cortex ($p \leq 0.05$, Student's *t* test); for the sake of clarity, these significant differences have not been marked by a symbol in the figure.

lular metabolic processes (nucleic acid, phosphate, and cholesterol metabolic processes), gene expression (transcription factors and nuclear receptors), apoptosis, synaptic plasticity, and blood vessel morphogenesis, among others (Table 4). Some signaling pathways were also overrepresented, such as the mitogen-activated protein kinase (MAPK) and the platelet-derived growth factor (PDGF) receptor signaling pathways (Table 5). With a similar analysis of 288 randomly selected genes (25 iterations), we obtained 29.9 ± 10.7 significantly enriched GO terms and 3.0 ± 1.7 functional clusters, indicating a false-positive rate of ~10%. The GO enrichment and functional clustering analysis indicates that many of the EE-induced changes in gene expression are involved in general cellular processes, including cell growth and differentiation, regulation of transcription, and several metabolic processes. In addition, overrepresented clusters include functional categories related to synaptic plasticity, strongly linking our findings at the molecular level to EE-induced anatomical and physiological changes in rat barrel cortex (Fox, 2002; Polley et al., 2004).

In situ hybridization of selected genes reveals cortical layer-specific patterning of mRNA expression

To study the expression patterns of EE-induced genes at the cellular level, *in situ* hybridization was performed for selected genes. This information will reveal in which cortical layers these genes are expressed and, more specifically, link the time-specific induction of these genes with specific locations in the cortical network of the barrel cortex. From the list of differentially expressed genes, we selected nine differentially expressed genes based on (1) qPCR validation, (2) strong regulation on EE (high FC), (3) different peaks of activation (0 h, 4 h, or both time points), and (4) different functional annotations. Included were genes previously known to be involved in neuronal plasticity and neuronal activation, such as the transcription factors *Fos* and *Egr3*, the cytoskeletal protein *Arc*, the nuclear factor *Nr4a2*, and the protein neuronal pentraxin 2 (*Nptx2*, also known as *Narp*, for neuronal activity-regulated protein). In addition, the vascular-related protein apolipoprotein L domain containing 1 (*Apold1*, also known as *Verge*, for vascular early response gene protein), the antiproliferative protein *Btg2*, the enzyme *Ch25h* (cholesterol metabolism), and the heparin-binding protein cysteine-rich angiogenic inducer 61 (*Cyr61*) were selected for *in situ* hybridization analysis.

The immediate-early gene and transcription factor *Fos* has been used extensively as a marker of neuronal activation (Sheng and Greenberg, 1990; Curran and Morgan, 1995). We used this marker to examine the main brain areas that were activated on EE exposure at $t = 0$ h. In addition to cerebral cortex, we found evidence of activity in striatum, hippocampus, and cerebellar cortex, all areas strongly associated with locomotor activity and spatial learning (Fig. 2). Interestingly, in stress-related areas such as the hypothalamic paraventricular nucleus and the amygdala, the *Fos* transcript was undetectable (data not shown), indicating low stress levels in these animals (most likely because of the habituation of the animals preceding EE). In addition, we investigated the expression of the other eight selected genes in cerebral cortex, striatum, hippocampus, and cerebellum (Fig. 2). Unfortunately, *Apold1* expression was below detection levels (data not shown); note that detection of *Apold1* also failed in the Allen Mouse Brain Atlas (Lein et al., 2007). For the remaining seven

genes, specific expression was detected in at least one of the time points studied, and all negative controls (sense probes) failed to detect any specific signal. Interestingly, whereas all seven genes were responsive to EE in the cerebral (barrel) cortex, each gene had a specific expression pattern in the other brain areas. Some genes (*Arc*, *Btg2*, *Cyr61*, and *Nptx2*) were upregulated in all areas except cerebellum, *Nr4a2* in all areas except striatum, *Egr3* in striatum and cortex, and *Ch25h* in cortex only.

We next focused on the patterns of mRNA expression of the selected genes in the different cortical layers of the barrel cortex (Fig. 3). *Fos* and *Ch25h* were undetectable in CTR groups; *Fos* was rapidly and strongly upregulated after EE at $t = 0$ h, whereas *Ch25h* levels increased only slightly at this time point. Interestingly, *Fos* levels were primarily increased in layers 2/3 and 4 and less in layers 5 and 6, whereas *Ch25h* levels increased similarly in all cortical layers. The two genes returned to basal (undetectable) levels at $t = 4$ h. Expression of *Btg2*, *Cyr61*, *Egr3*, and *Nr4a2* was barely detectable in CTR animals; only residual to low levels in scattered cells were detected primarily in layer 2/3 (*Btg2*, *Egr3*), layer 6 (*Cyr61*), or both layers 2/3 and 6 (*Nr4a2*). EE-induced upregulation of *Egr3* was observed at both $t = 0$ h and $t = 4$ h and took place primarily in layers 2/3 and 6 and to a lesser extent in layers 4 and 5. In contrast, *Btg2* and *Cyr61* and *Nr4a2* were only upregulated at $t = 0$ h. At this time point, *Btg2*-positive cells increased in layers 2/3, 6, and, to a lesser extent, 4 and 5, whereas *Cyr61* increased primarily in layer 6. *Nr4a2* was strongly increased in layers 2/3 and 4 and less in layers 5 and 6. The plasticity-related genes *Arc* and *Nptx2* displayed a clear expression already in the CTR groups. Whereas *Arc* was primarily expressed in layers 4 and 6 and less in layers 2/3 and 5, *Nptx2* levels were detected to an equal extent in layers 2/3, 5, and 6. During EE exposure, *Arc* levels were upregulated in all cortical layers, except layer 1 at $t = 0$ h, and returned to basal levels at $t = 4$ h. In contrast, *Nptx2* levels did not increase during EE at $t = 0$ h but did increase dramatically at $t = 4$ h, especially in layer 2/3 and also layers 5 and 6.

Expression levels were comparable in both brain hemispheres for all the expression patterns described above. In summary, the *in situ* hybridization results show time- and layer-specific molecular changes related to experience-induced plasticity in the barrel cortex.

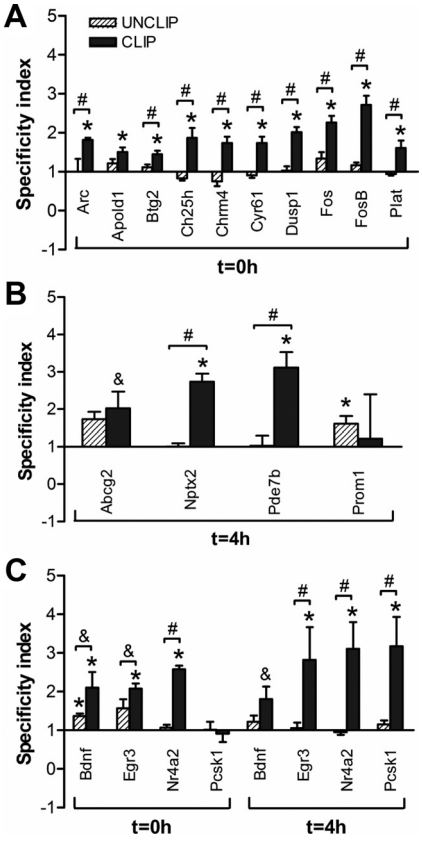

Figure 8. Specificity index showing the right/left ratio of activation in the two hemispheres of UNCLIP and CLIP groups. A specificity index was calculated, based on qPCR data, to explore the degree of activation of the genes selected for qPCR validation in right (R) versus left (L) barrel cortices (for details, see Materials and Methods). In CLIP animals, if the index is higher than 1, activation is higher in spared (R) than in deprived (L) cortex. In UNCLIP animals, the specificity index quantifies hemispheric differences in the absence of clipping. Shown are the results of this index for genes specifically regulated after EE at $t = 0$ h (***A***), $t = 4$ h (***B***), or both time points (***C***) (bottom). Bars represent average specificity index values ± SEM. * represents values significantly higher than 1 (one-sample *t* test, reference value 1, $p \leq 0.05$). # represents significant differences between UNCLIP and CLIP groups ($p \leq 0.05$, Student's *t* test). Marginally significant differences are indicated by & symbol ($0.05 < p \leq 0.1$).

EE-induced mRNA expression changes in the barrel cortex are attributable to differential somatosensory processing

Because EE is known to induce plasticity in the entire brain, we investigated whether the changes in mRNA expression at the level of the barrel cortex reflected specific modifications in somatosensory processing or simply reflected general cortical activation. For this purpose, we performed experiments not only in rats without whisker manipulation (UNCLIP group) but also with rats in which the whiskers had been removed unilaterally 18 h before the EE session (CLIP group). Importantly, we performed a behavioral analysis showing that such a short time of deprivation did not affect exploratory behavior in CLIP animals because, similar to UNCLIP rats, CLIP animals spent most of the time actively whisking rather than displaying the other behaviors (two-way ANOVA, $p \leq 0.0001$; SNK) (Fig. 4), and they had no preference for a particular location in the test cage (data not shown). We then performed detailed qPCR analysis of the 18 differentially expressed and validated genes selected on the basis of the microarray results (see above) and compared the expression levels in the spared versus the deprived sides of the barrel cortex. The direction (up or down) and time point ($t = 0$ h or $t = 4$ h) of the changes in expression determined by qPCR were the same as those found by microarray analysis and were similar between UNCLIP and CLIP groups. Indeed, we observed for a number of genes significant upregulation after EE at $t = 0$ h (Fig. 5, *Arc*, *Apold1*, *Btg2*, *Ch25h*, *Chrm4*, *Cyr61*, *Dusp1*, *Fos*, *FosB*, and *Plat*), at $t = 4$ h (Fig. 6, *Nptx2* and phosphodiesterase 7B, *Pde7b*), or at both time points (Fig. 7, *Bdnf*, *Egr3*, *Nr4a2*, and *Pcsk1*) and significant downregulation at $t = 4$ h (Fig. 6, ABC transporter G2, *Abcg2*) (two-way ANOVA, followed by SNK *post hoc* tests, $p \leq 0.05$). Only prominin 1 (Fig. 6, *Prom1*), which was significantly downregulated at $t = 4$ h in UNCLIP animals, did not show significant differences in CLIP animals. Importantly, when compared with UNCLIP animals, EE-induced changes in gene expression in CLIP groups were more prominent in the spared (R side) than in the deprived (L side) barrel cortex (Student's *t* test, $p \leq 0.05$). However, for most genes, there was residual activation in the deprived side (when comparing L side of EE animals with respect to CTR animals, Student's *t* test, $p \leq 0.05$). To quantify and statistically test the specificity of the effects in the spared side, we computed a specificity index for each gene. The index was defined as the ratio of the difference between EE and CTR expression levels in spared versus deprived side (Fig. 8). As expected, in

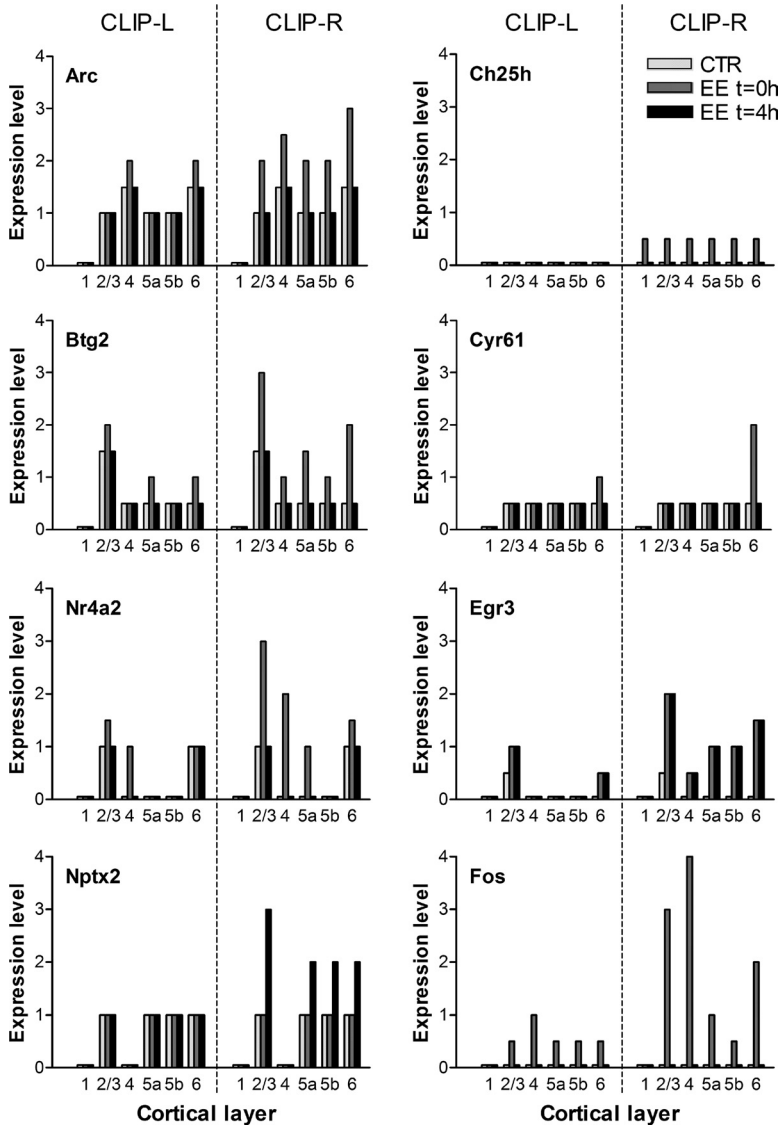

Figure 9. EE-induced layer-specific differential gene expression in the rat barrel cortex of CLIP groups. *In situ* hybridization analysis showing expression levels of selected genes in the barrel cortex, namely *Arc*, *Btg2*, *Ch25h*, *Cyr61*, *Egr3*, *Fos*, *Nptx2*, and *Nr4a2*. Expression levels were evaluated in CLIP animals, under CTR, EE $t = 0$ h, and EE $t = 4$ h conditions. The analysis was performed separately for left (L, deprived) and right (R, spared) barrel cortices. Note that the expression levels in the R barrel cortex were similar as in UNCLIP animals and that L barrel cortex only displayed residual activation.

CLIP groups, the specificity index was significantly higher than 1 for most genes tested (Student's one-sample *t* test, reference value 1, $p \leq 0.05$) (Fig. 8), indicating that in these groups the degree of activation in the spared side was substantially higher than in the deprived side. Similar results were found by *in situ* hybridization, showing only residual activation in the deprived side and prominent activation in the spared side (Fig. 9). These observations support the view that EE-induced changes in gene expression observed by microarray analysis at the level of the barrel cortex are specific for changes in sensory processing and do not merely reflect general changes in cortical activity.

Discussion

Using microarray mRNA expression profiling, we have provided a comprehensive view on the genes induced in the adult rat barrel cortex by sensory experience. The involvement of these genes in the processing of somatosensory information was supported by studying selected genes at a cellular (cortical layer) level and validating the results in deprived versus spared barrel cortices of whisker-clipped animals. Differentially expressed genes are involved in metabolic processes, regulation of transcription, and intracellular cascades such as PDGF and MAPK signaling pathways, but also in the regulation of synaptic plasticity and blood vessel morphogenesis. This is the first time that a genomewide study is applied at the level of the barrel cortex. Remarkably, the genes found to be differentially expressed in our study hardly overlap with those found by microarray analysis of whole cortex of adult EE-exposed mice (Rampon et al., 2000), possibly as a result of differences in experimental design (e.g., stress levels, length of EE exposure, timing of when the animals were killed, tissue and species used). Interestingly, some genes from our study do overlap with genes known to be regulated by sensory experience in rodent barrel cortex, such as *Bdnf*, *Crem*, *Egr1*, *Fos*, *FosB*, and *JunB* (Rocamora et al., 1996; Pinaud et al., 2006). Our results also overlap, at least partly, with other genomewide studies in related models of experience-induced plasticity. For instance, in the visual cortex, a 4 d mononuclear deprivation at the peak of the critical period induced differential expression of genes also found in our dataset, namely *Bdnf*, *Btg2*, *FosB*, *Insig1*, *Nptx2*, and *Pdgfb* (Tropea et al., 2006). Strikingly, in the same model, a set of genes (*Bdnf*, *Dusp1*, *Dusp6*, *Egr1*, *Egr2*, *Fos*, *FosB*, *Gadd45b*, *Ier2*, *JunB*, and *Nr4a1*) is regulated independently of the developmental stage (Majdan and Shatz, 2006), and in the barrel cortex, we found that these MAPK signaling pathway components were also regulated by experience. Moreover, during singing behavior, some of these genes were also differentially expressed in the songbird brain (Wada et al., 2006; Dong et al., 2009), supporting their involvement in experience-dependent plasticity in the non-mammalian brain as well.

By studying gene expression at the level of the barrel cortex and validating the results by combining EE with whisker clipping, showing strong EE-induced mRNA expression in spared barrel cortex (contralateral to clipping), we have obtained information on genes involved in the processing of somatosensory input. However, although to a much smaller extent, differential expression was still observed in deprived barrel cortex (ipsilateral to clipping), suggesting residual processing of somatosensory input in the deprived hemisphere. This could be attributable to several reasons. First, because whisker clipping leaves the whisker follicles intact, whiskers may still have transmitted sensory information during attempted whisking attributable to follicle stimulation. Second, passive activation attributable to skin contact may have effects similar to passive whisker deflections, which are known to cause postsynaptic potentials in the ipsilateral barrel, although with smaller amplitudes and longer latencies (Manns et al., 2004). Third, it is possible that activation from the spared cortex can

spread to the contralateral side via callosal projections. The paralemniscal pathway has strong interhemispheric connections (Li and Ebner, 2006), conveys information about the temporal frequency of whisker movements (Ahissar et al., 2000), and is involved in the sensorimotor control of whisker movement by providing reference signals during object recognition (Yu et al., 2006). Such information could be relevant in an EE in which several novel stimuli are present, possibly leading to a highly active paralemniscal pathway and the observed residual processing.

Sensory experiences and the resulting synaptic activity are critical for the shaping of neuronal networks in the barrel cortex. Several processes, including dendritic branching, synaptogenesis, maturation, and elimination of synapses, lie at the base of this shaping (Flavell and Greenberg, 2008). Transcription precedes experience-dependent plasticity by regulating the expression of several downstream genes that subsequently modulate synaptic properties. In fact, many of the transcription factor genes detected in our microarray analysis have been linked previously to synaptic plasticity, in either the barrel cortex or other brain regions. For instance, *Btg2* is involved in neuronal differentiation (Bradbury et al., 1991) and plays a crucial role in contextual memory (Farioli-Vecchioli et al., 2008, 2009). The upregulation of *Crem* during EE confirms previous observations, also in barrel cortex (Bisler et al., 2002), supporting its key role in neuronal plasticity (Mioduszewska et al., 2003). *Fos* and *Jun* induce expression of *Bdnf* (Zhang et al., 2002), one of the pivotal molecules in neuronal plasticity (Greenberg et al., 2009). In the barrel cortex, Bdnf regulates the balance between excitatory and inhibitory neurotransmitter systems (Genoud et al., 2004) and was also upregulated in our study, together with two of its processing enzymes, *Pcsk1* (Seidah and Chrétien, 1999) and *Plat* (Pang et al., 2004). Interestingly, Bdnf activation increases expression of *Egr3* (Roberts et al., 2006), which is involved in short-term memory (Poirier et al., 2008). Egr3 has been shown to induce expression of *Arc*, which is essential for long-term potentiation (LTP) persistence (Li et al., 2005). EE upregulates *Arc* expression in rat barrel cortex and hippocampus (Ramírez-Amaya et al., 2005). Finally, all members of the inducible orphan nuclear receptor family of transcription factors (*Nr4a1*, *Nr4a2*, and *Nr4a3*) were also upregulated during EE. This, together with their implication in neuronal development (Perlmann and Wallén-Mackenzie, 2004) and responsiveness to depolarization (Lam et al., 2010), suggests a key role for these transcription factors in experience-dependent plasticity.

Apart from transcription factors, the MAPK and PDGF receptor signaling pathways were also significantly regulated during enrichment, as evidenced by the GO analysis. Activation of the MAPK pathway by glutamate receptors has been associated with synaptic plasticity (Wang et al., 2007). The phosphatases *Dusp1* and *Dusp6* were both upregulated by EE; *Dusp1* targets the MAPK pathway (Farooq and Zhou, 2004) and is in turn inhibited by *Dusp6* (Vogt et al., 2005). Given that a short activation of the MAPK pathway is enough to ensure LTP (Wang et al., 2007), expression of these phosphatases probably serves to fine tune the activation of this signaling cascade and overcome detrimental effects of sustained cellular activation. As to the PDGF-B receptor signaling pathway, recent studies suggest that PDGF-B plays a role in regulating NMDA receptor excitability (Egawa-Tsuzuki et al., 2004) and that PDGF-B is also able to induce *Arc* expression (Peng et al., 2010), linking this pathway to neuronal plasticity.

An intriguing finding in our study was the differential expression of genes related to blood vessel morphogenesis, namely *Cyr61* and *Apold1*. *Cyr61* is important for extracellular matrix production (Chen and Du, 2007) and is under the control of muscarinic acetylcholine receptor (Chrm) signaling in cortical neurons (Albrecht et al., 2000); interestingly, *Chrm4* was also upregulated in our study. The possible reorganization of neural networks in barrel cortex may increase the need for energy supply and thus for the formation of novel blood vessels in which *Cyr61* could be of central importance. This could hold for *Apold1* as well, which regulates the differentiation of brain endothelial cells and has been shown to respond to seizures and hypoxia in brain vasculature (Regard et al., 2004). Genes involved in cholesterol biosynthesis, shown to be expressed in neuronal cells (Valdez et al., 2010), such as *Ch25h* or *Hmgcr*, were also differentially expressed. The link between cholesterol turnover, LTP, and learning has been established previously (Kotti et al., 2006), and more recently the activity of presynaptic protein kinases has been found to be sensitive to changes in membrane cholesterol content (Smith et al., 2010).

Finally, although not clearly overrepresented in a particular functional category, *Ptgs2* and *Nptx2* have also been linked previously to neuronal plasticity. For instance, *Ptgs2* plays a crucial role in the modulation of hippocampal synaptic transmission and plasticity by regulating prostaglandin signaling (Sang and Chen, 2006). *Nptx2* overexpression induces the formation of excitatory synapses (O'Brien et al., 1999) and clustering of AMPA receptors *in vitro* (Fox and Umemori, 2006).

In addition to knowledge about their functional background, knowing the timing and cellular expression patterns of the differentially expressed genes is crucial to understand their role in S1 plasticity. Our detailed analysis of selected genes indicates that both input (layer 4) and output layers are activated early after EE. For instance, at $t = 0$ h, *Fos* and *Nr4a2* are activated in input and output layers, whereas *Btg2* is primarily activated in output layers. In contrast, at later time points, mainly output layers are activated, as evidenced from the *Egr3* and *Nptx2* expression patterns at $t = 4$ h. These findings suggest that initial gene activation would reflect changes in presynaptic and postsynaptic neurons in S1, whereas later in time it would reflect postsynaptic changes. Interestingly, changes in layer 2/3, the most plastic layer in adult barrel cortex (Fox, 2002), seem to be more long lasting, linking gene expression to neuronal plasticity.

In summary, we show that, *in vivo*, somatosensory processing in the rat barrel cortex activates a wide variety of genes in a time- and layer-specific manner. Thus, the present data provide a solid experimental framework for future genetic, electrophysiological, and imaging studies that will give insight into the mechanisms underlying experience-dependent reorganization of sensory systems.

References

Ahissar E, Sosnik R, Haidarliu S (2000) Transformation from temporal to rate coding in a somatosensory thalamocortical pathway. Nature 406:302–306.

Albrecht C, von Der Kammer H, Mayhaus M, Klaudiny J, Schweizer M, Nitsch RM (2000) Muscarinic acetylcholine receptors induce the expression of the immediate early growth regulatory gene CYR61. J Biol Chem 275:28929–28936.

Aronoff R, Petersen CC (2008) Layer, column and cell-type specific genetic manipulation in mouse barrel cortex. Front Neurosci 2:64–71.

Barth AL, McKenna M, Glazewski S, Hill P, Impey S, Storm D, Fox K (2000) Upregulation of cAMP response element-mediated gene expression during experience-dependent plasticity in adult neocortex. J Neurosci 20:4206–4216.

Bisler S, Schleicher A, Gass P, Stehle JH, Zilles K, Staiger JF (2002) Expression of c-Fos, ICER, Krox-24 and JunB in the whisker-to-barrel pathway

of rats: time course of induction upon whisker stimulation by tactile exploration of an enriched environment. J Chem Neuroanat 23:187–198.
Bonefeld BE, Elfving B, Wegener G (2008) Reference genes for normalization: a study of rat brain tissue. Synapse 62:302–309.
Bradbury A, Possenti R, Shooter EM, Tirone F (1991) Molecular cloning of PC3, a putatively secreted protein whose mRNA is induced by nerve growth factor and depolarization. Proc Natl Acad Sci U S A 88:3353–3357.
Brecht M (2007) Barrel cortex and whisker-mediated behaviors. Curr Opin Neurobiol 17:408–416.
Brecht M, Fee MS, Garaschuk O, Helmchen F, Margrie TW, Svoboda K, Osten P (2004) Novel approaches to monitor and manipulate single neurons *in vivo*. J Neurosci 24:9223–9227.
Chen Y, Du XY (2007) Functional properties and intracellular signaling of CCN1/Cyr61. J Cell Biochem 100:1337–1345.
Curran T, Morgan JI (1995) Fos: an immediate-early transcription factor in neurons. J Neurobiol 26:403–412.
Dennis G Jr, Sherman BT, Hosack DA, Yang J, Gao W, Lane HC, Lempicki RA (2003) DAVID: database for annotation, visualization, and integrated discovery. Genome Biol 4:P3.
Diamond ME, von Heimendahl M, Knutsen PM, Kleinfeld D, Ahissar E (2008) "Where" and "what" in the whisker sensorimotor system. Nat Rev Neurosci [Erratum (2008) 9:709] 9:601–612.
Dong S, Replogle KL, Hasadsri L, Imai BS, Yau PM, Rodriguez-Zas S, Southey BR, Sweedler JV, Clayton DF (2009) Discrete molecular states in the brain accompany changing responses to a vocal signal. Proc Natl Acad Sci U S A 106:11364–11369.
Egawa-Tsuzuki T, Ohno M, Tanaka N, Takeuchi Y, Uramoto H, Faigle R, Funa K, Ishii Y, Sasahara M (2004) The PDGF B-chain is involved in the ontogenic susceptibility of the developing rat brain to NMDA toxicity. Exp Neurol 186:89–98.
Farioli-Vecchioli S, Saraulli D, Costanzi M, Pacioni S, Cinà I, Aceti M, Micheli L, Bacci A, Cestari V, Tirone F (2008) The timing of differentiation of adult hippocampal neurons is crucial for spatial memory. PLoS Biol 6:e246.
Farioli-Vecchioli S, Saraulli D, Costanzi M, Leonardi L, Cinà I, Micheli L, Nutini M, Longone P, Oh SP, Cestari V, Tirone F (2009) Impaired terminal differentiation of hippocampal granule neurons and defective contextual memory in PC3/Tis21 knockout mice. PloS One 4:e8339.
Farooq A, Zhou MM (2004) Structure and regulation of MAPK phosphatases. Cell Signal 16:769–779.
Feldman DE, Brecht M (2005) Map plasticity in somatosensory cortex. Science 310:810–815.
Filipkowski RK, Rydz M, Kaczmarek L (2001) Expression of c-Fos, Fos B, Jun B, and Zif268 transcription factor proteins in rat barrel cortex following apomorphine-evoked whisking behavior. Neuroscience 106:679–688.
Flavell SW, Greenberg ME (2008) Signaling mechanisms linking neuronal activity to gene expression and plasticity of the nervous system. Annu Rev Neurosci 31:563–590.
Fox K (2002) Anatomical pathways and molecular mechanisms for plasticity in the barrel cortex. Neuroscience 111:799–814.
Fox MA, Umemori H (2006) Seeking long-term relationship: axon and target communicate to organize synaptic differentiation. J Neurochem 97:1215–1231.
Genoud C, Knott GW, Sakata K, Lu B, Welker E (2004) Altered synapse formation in the adult somatosensory cortex of brain-derived neurotrophic factor heterozygote mice. J Neurosci 24:2394–2400.
Genoud C, Quairiaux C, Steiner P, Hirling H, Welker E, Knott GW (2006) Plasticity of astrocytic coverage and glutamate transporter expression in adult mouse cortex. PLoS Biol 4:e343.
Greenberg ME, Xu B, Lu B, Hempstead BL (2009) New insights in the biology of BDNF synthesis and release: implications in CNS function. J Neurosci 29:12764–12767.
Harwell C, Burbach B, Svoboda K, Nedivi E (2005) Regulation of cpg15 expression during single whisker experience in the barrel cortex of adult mice. J Neurobiol 65:85–96.
Huang da W, Sherman BT, Lempicki RA (2009) Systematic and integrative analysis of large gene lists using DAVID bioinformatics resources. Nat Protoc 4:44–57.
Huber D, Petreanu L, Ghitani N, Ranade S, Hromádka T, Mainen Z, Svoboda K (2008) Sparse optical microstimulation in barrel cortex drives learned behaviour in freely moving mice. Nature 451:61–64.
Ishibashi H (2002) Increased synaptophysin expression through whisker stimulation in rat. Cell Mol Neurobiol 22:191–195.
Knott G, Holtmaat A (2008) Dendritic spine plasticity–current understanding from in vivo studies. Brain Res Rev 58:282–289.
Korosi A, Veening JG, Kozicz T, Henckens M, Dederen J, Groenink L, van der Gugten J, Olivier B, Roubos EW (2006) Distribution and expression of CRF receptor 1 and 2 mRNAs in the CRF over-expressing mouse brain. Brain Res 1072:46–54.
Kotti TJ, Ramirez DM, Pfeiffer BE, Huber KM, Russell DW (2006) Brain cholesterol turnover required for geranylgeraniol production and learning in mice. Proc Natl Acad Sci U S A 103:3869–3874.
Lam BY, Zhang W, Ng DC, Maruthappu M, Roderick HL, Chawla S (2010) CREB-dependent Nur77 induction following depolarization in PC12 cells and neurons is modulated by MEF2 transcription factors. J Neurochem 112:1065–1073.
Lein ES, Hawrylycz MJ, Ao N, Ayres M, Bensinger A, Bernard A, Boe AF, Boguski MS, Brockway KS, Byrnes EJ, Chen L, Chen L, Chen TM, Chin MC, Chong J, Crook BE, Czaplinska A, Dang CN, Datta S, Dee NR, et al. (2007) Genome-wide atlas of gene expression in the adult mouse brain. Nature 445:168–176.
Li L, Ebner FF (2006) Balancing bilateral sensory activity: callosal processing modulates sensory transmission through the contralateral thalamus by altering the response threshold. Exp Brain Res 172:397–415.
Li L, Carter J, Gao X, Whitehead J, Tourtellotte WG (2005) The neuroplasticity-associated arc gene is a direct transcriptional target of early growth response (Egr) transcription factors. Mol Cell Biol 25:10286–10300.
Majdan M, Shatz CJ (2006) Effects of visual experience on activity-dependent gene regulation in cortex. Nat Neurosci 9:650–659.
Manns ID, Sakmann B, Brecht M (2004) Sub- and suprathreshold receptive field properties of pyramidal neurones in layers 5A and 5B of rat somatosensory barrel cortex. J Physiol 556:601–622.
Mioduszewska B, Jaworski J, Kaczmarek L (2003) Inducible cAMP early repressor (ICER) in the nervous system: a transcriptional regulator of neuronal plasticity and programmed cell death. J Neurochem 87:1313–1320.
O'Brien RJ, Xu D, Petralia RS, Steward O, Huganir RL, Worley P (1999) Synaptic clustering of AMPA receptors by the extracellular immediate-early gene product Narp. Neuron 23:309–323.
Pang PT, Teng HK, Zaitsev E, Woo NT, Sakata K, Zhen S, Teng KK, Yung WH, Hempstead BL, Lu B (2004) Cleavage of proBDNF by tPA/plasmin is essential for long-term hippocampal plasticity. Science 306:487–491.
Paxinos G, Watson C (1998) The rat brain in stereotaxic coordinates. San Diego: Academic.
Peng F, Yao H, Bai X, Zhu X, Reiner BC, Beazely M, Funa K, Xiong H, Buch S (2010) Platelet-derived growth factor-mediated induction of the synaptic plasticity gene Arc/Arg3.1. J Biol Chem 285:21615–21624.
Perlmann T, Wallén-Mackenzie A (2004) Nurr1, an orphan nuclear receptor with essential functions in developing dopamine cells. Cell Tissue Res 318:45–52.
Petersen CC (2007) The functional organization of the barrel cortex. Neuron 56:339–355.
Petersen CC (2009) Genetic manipulation, whole-cell recordings and functional imaging of the sensorimotor cortex of behaving mice. Acta Physiol (Oxf) 195:91–99.
Petreanu L, Mao T, Sternson SM, Svoboda K (2009) The subcellular organization of neocortical excitatory connections. Nature 457:1142–1145.
Pinaud R, Filipkowski RK, Fortes AF, Tremere LA (2006) Immediate early gene expression in the primary somatosensory cortex: focus on the barrel cortex. In: Immediate early genes in sensory processing, cognitive performance and neurological disorders (Pinaud R, Tremere LA, eds), pp 73–92. New York: Springer Science + Business Media.
Poirier R, Cheval H, Mailhes C, Garel S, Charnay P, Davis S, Laroche S (2008) Distinct functions of egr gene family members in cognitive processes. Front Neurosci 2:47–55.
Polley DB, Kvasnák E, Frostig RD (2004) Naturalistic experience transforms sensory maps in the adult cortex of caged animals. Nature 429:67–71.
Ramírez-Amaya V, Vazdarjanova A, Mikhael D, Rosi S, Worley PF, Barnes CA (2005) Spatial exploration-induced Arc mRNA and protein expression: evidence for selective, network-specific reactivation. J Neurosci 25:1761–1768.
Rampon C, Jiang CH, Dong H, Tang YP, Lockhart DJ, Schultz PG, Tsien JZ,

Hu Y (2000) Effects of environmental enrichment on gene expression in the brain. Proc Natl Acad Sci U S A 97:12880–12884.
Regard JB, Scheek S, Borbiev T, Lanahan AA, Schneider A, Demetriades AM, Hiemisch H, Barnes CA, Verin AD, Worley PF (2004) Verge: a novel vascular early response gene. J Neurosci 24:4092–4103.
Roberts DS, Hu Y, Lund IV, Brooks-Kayal AR, Russek SJ (2006) Brain-derived neurotrophic factor (BDNF)-induced synthesis of early growth response factor 3 (Egr3) controls the levels of type A GABA receptor alpha 4 subunits in hippocampal neurons. J Biol Chem 281:29431–29435.
Rocamora N, Welker E, Pascual M, Soriano E (1996) Upregulation of BDNF mRNA expression in the barrel cortex of adult mice after sensory stimulation. J Neurosci 16:4411–4419.
Sang N, Chen C (2006) Lipid signaling and synaptic plasticity. Neuroscientist 12:425–434.
Schaeren-Wiemers N, Gerfin-Moser A (1993) A single protocol to detect transcripts of various types and expression levels in neural tissue and cultured cells: in situ hybridization using digoxigenin-labelled cRNA probes. Histochemistry 100:431–440.
Schubert D, Kötter R, Staiger JF (2007) Mapping functional connectivity in barrel-related columns reveals layer- and cell type-specific microcircuits. Brain Struct Funct 212:107–119.
Seidah NG, Chrétien M (1999) Proprotein and prohormone convertases: a family of subtilases generating diverse bioactive polypeptides. Brain Res 848:45–62.
Sheng M, Greenberg ME (1990) The regulation and function of c-fos and other immediate early genes in the nervous system. Neuron 4:477–485.
Smith AJ, Sugita S, Charlton MP (2010) Cholesterol-dependent kinase activity regulates transmitter release from cerebellar synapses. J Neurosci 30:6116–6121.
Spruijt BM, van Hooff JA, Gispen WH (1992) Ethology and neurobiology of grooming behavior. Physiol Rev 72:825–852.
Tropea D, Kreiman G, Lyckman A, Mukherjee S, Yu H, Horng S, Sur M (2006) Gene expression changes and molecular pathways mediating activity-dependent plasticity in visual cortex. Nat Neurosci 9:660–668.
Tusher VG, Tibshirani R, Chu G (2001) Significance analysis of microarrays applied to the ionizing radiation response. Proc Natl Acad Sci U S A 98:5116–5121.
Valdez CM, Smith MA, Perry G, Phelix CF, Santamaria F (2010) Cholesterol homeostasis markers are localized to mouse hippocampal pyramidal and granule layers. Hippocampus 20:902–905.
Vandesompele J, De Preter K, Pattyn F, Poppe B, Van Roy N, De Paepe A, Speleman F (2002) Accurate normalization of real-time quantitative RT-PCR data by geometric averaging of multiple internal control genes. Genome Biol 3:RESEARCH0034.
Vogt A, Tamewitz A, Skoko J, Sikorski RP, Giuliano KA, Lazo JS (2005) The benzo[c]phenanthridine alkaloid, sanguinarine, is a selective, cell-active inhibitor of mitogen-activated protein kinase phosphatase-1. J Biol Chem 280:19078–19086.
Wada K, Howard JT, McConnell P, Whitney O, Lints T, Rivas MV, Horita H, Patterson MA, White SA, Scharff C, Haesler S, Zhao S, Sakaguchi H, Hagiwara M, Shiraki T, Hirozane-Kishikawa T, Skene P, Hayashizaki Y, Carninci P, Jarvis ED (2006) A molecular neuroethological approach for identifying and characterizing a cascade of behaviorally regulated genes. Proc Natl Acad Sci U S A 103:15212–15217.
Wang JQ, Fibuch EE, Mao L (2007) Regulation of mitogen-activated protein kinases by glutamate receptors. J Neurochem 100:1–11.
Woolsey TA, Van der Loos H (1970) The structural organization of layer IV in the somatosensory region (SI) of mouse cerebral cortex. The description of a cortical field composed of discrete cytoarchitectonic units. Brain Res 17:205–242.
Yu C, Derdikman D, Haidarliu S, Ahissar E (2006) Parallel thalamic pathways for whisking and touch signals in the rat. PLoS Biol 4:e124.
Zhang J, Zhang D, McQuade JS, Behbehani M, Tsien JZ, Xu M (2002) c-fos regulates neuronal excitability and survival. Nat Genet 30:416–420.